

Université du Québec
Institut national de la recherche scientifique
Énergie Matériaux Télécommunications

Maximum Likelihood SNR Estimation of
Linearly-Modulated Signals over Time-Varying
Flat-Fading SIMO Channels Using the
Expectation-Maximization Concept

Par
Rabii Meftahi

Mémoire présenté
pour l'obtention
du grade de Maitre ès sciences (M.Sc) en télécommunications

Jury d'évaluation

Directeur de recherche

Sofiène Affes, INRS-ÉMT

Examineur interne

Le Long, INRS-ÉMT

Examineur externe

Paul Fortier,
Département de génie électrique et de génie
informatique, Université Laval

Acknowledgements

I wish to thank Prof. Sofiène Affes for giving me the opportunity to work in his team, and for guiding me throughout my MSc program. His remarks as well as his pertinent criticism led me to the right path.

I want also to thank Mr. Faouzi Bellili for all his effort, for being there for me, providing me with valuable advices and providing the perfect example for me for my research career.

A special thanks to the external and internal jury members, Prof. Paul Fortier, from Université Laval and Prof. Le Long from INRS-ÉMT who have kindly accepted to assess my MSc thesis. I want to express my thanks and gratitude to all my family, for their patience, and for all their encouragements.

Finally, I want to thank all my colleagues and all the staff at INRS, for providing a perfect environment, and for making me feel as if I was surrounded by my family members...

Abstract

In this thesis, we tackle the problem of maximum likelihood (ML) estimation of the signal-to-noise ratio (SNR) parameter over time-varying single-input multiple-output (SIMO) channels, for both data-aided (DA) and non-data-aided (NDA) scenarios. Unlike classical techniques where the channel is assumed to be slowly time-varying and therefore considered as constant over the entire observation period, we address the more challenging problem of *instantaneous* SNR estimation over fast time-varying channels. The channel variations are locally tracked using a polynomial-in-time expansion. First, we derive in closed-form expressions the DA ML estimator along with its bias. The latter is subsequently subtracted in order to obtain a new unbiased estimator whose variance and the corresponding Cramér-Rao lower bound (CRLB) are also derived in closed-form. Due to the extreme nonlinearity of the log-likelihood function in the NDA case, we resort to the expectation-maximization (EM) technique to iteratively obtain the exact NDA ML SNR estimates within very few iterations. The new estimators are able to accurately estimate the *instantaneous* per-antenna SNRs over a wide practical SNR range. In particular, the new NDA ML estimator exhibits a substantial performance advantage against the *WGL* technique [4], the only suitable benchmark available in the literature so far on SNR estimation over time-varying channels, not only in

its original single-input single-output (SISO) version but also against its SIMO extension that is derived and detailed later in this thesis.

Chapter 1

Résumé

Dans ce mémoire, nous proposons un estimateur de maximum de vraisemblance (ML) du rapport signal sur bruit (SNR) pour les canaux variant dans le temps dans les systèmes à entrée unique et à sorties multiples (SIMO), non seulement dans le cas assisté par signaux pilotes (DA), mais aussi dans le scénario autodidacte de données inconnues (NDA). Contrairement aux techniques classiques où le canal est supposé être lentement variable dans le temps et donc considérée comme constant sur toute la période d'observation, nous abordons le problème d'estimation du SNR instantané pour les canaux fortement variables dans le temps. Les variations du canal sont localement suivies en utilisant une expansion polynomiale en temps. Tout d'abord, nous dérivons d'une manière analytiquement exacte l'estimateur ML du SNR, dans les deux cas DA et NDA aussi bien que la borne inférieure de Cramér-Rao correspondante (CRLB). Ensuite, en raison de la non-linéarité extrême de la fonction log-vraisemblance dans le cas NDA, nous avons recours à la technique "expectation-maximization" (EM) pour obtenir l'estimé ML exact du SNR, itérativement après un nombre

très réduit d'itérations. Les nouveaux estimateurs sont en mesure d'estimer avec précision notable les SNR instantanés par antenne sur une large plage du SNR. En particulier, le nouvel estimateur ML NDA présente un avantage substantiel en performance comparé au seul travail publié sur le sujet d'estimation du SNR sur canaux variables dans le temps, non seulement dans sa version originale à entrée et à sortie unique (SISO), mais aussi comparé à son extension SIMO qui est dérivée et détaillée plus loin dans ce mémoire.

1.1 Estimateur à maximum de vraisemblance

L'estimateur à maximum de vraisemblance (MLE) est un estimateur dit à efficacité asymptotique. Il est défini comme la valeur du paramètre qui maximise la fonction de vraisemblance. En général, lorsqu'il est non-biaisé, le MLE atteint asymptotiquement la borne de Cramér-Rao (CRLB) et son erreur possède une distribution Gaussienne. Dans notre cas, on cherche à estimer le rapport signal-à-bruit, en utilisant l'approche maximum de vraisemblance, pour les systèmes à entrée unique et à sorties multiples (SIMO), variables dans le temps.

La formulation du problème d'estimation varie suivant que nous considérons un signal à temps continu ou un signal à temps discret. La première approche semble être la plus appropriée à cause de la nature physique du signal, mais les récepteurs numériques opèrent sur des séquences échantillonnées.

Nous considérons d'abord une formulation à temps continue pour étendre, dans le chapitre qui suit, l'approche au temps discret. Nous notons par θ l'ensemble des paramètres inconnus qui inclut les coefficients du canal ainsi que la variance du bruit. Nous adoptons la notation

$x(t, \boldsymbol{\theta})$ pour le signal reçu en absence de bruit qui met en évidence la dépendance en $\boldsymbol{\theta}$. Le modèle en bande de base a l'*i*^{ème} antenne de réception est:

$$y_i(t) = x_i(t, \boldsymbol{\gamma}) + w_i(t), \quad (1.1)$$

où $w_i(t)$ est le bruit additif complexe. On considère que $y_i(t)$ est une réalisation d'un processus aléatoire $y_i(t)$ pour une valeur donnée de $\hat{\boldsymbol{\theta}} = \boldsymbol{\theta}$. En effet, une réalisation de $y_i(t)$ a un certain degré de ressemblance avec $y_i(t)$ dépendamment de la ressemblance entre $x_i(t, \hat{\boldsymbol{\theta}})$ et $x_i(t, \boldsymbol{\theta})$, en d'autres termes, la distance entre $\hat{\boldsymbol{\theta}}$ et $\boldsymbol{\theta}$. L'estimateur à maximum de vraisemblance est basé sur le calcul de $\hat{\boldsymbol{\theta}}$ de sorte que la ressemblance entre $y_i(t)$ et la réalisation $y_i(t)$ soit maximale. En termes de probabilité, nous appelons $p(y_i(t) | \hat{\boldsymbol{\theta}})$ la densité de probabilité de $y_i(t)$ conditionnée par $\hat{\boldsymbol{\theta}}$. Supposons que pour deux réalisations de $\hat{\boldsymbol{\theta}}$, notées par $\hat{\boldsymbol{\theta}}_1$ et $\hat{\boldsymbol{\theta}}_2$, nous avons:

$$p(y_i(t) = y_i(t) | \hat{\boldsymbol{\theta}}_1) < p(y_i(t) = y_i(t) | \hat{\boldsymbol{\theta}}_2), \quad (1.2)$$

alors $\hat{\boldsymbol{\theta}}_2$ est dit plus vraisemblable que $\hat{\boldsymbol{\theta}}_1$.

Comme nous l'avons mentionné, le but est de maximiser $p(y_i(t) = y_i(t) | \hat{\boldsymbol{\theta}})$ par rapport à $\hat{\boldsymbol{\theta}}$.

La position du maximum est appelée estimé à maximum de vraisemblance et est donnée par:

$$\hat{\boldsymbol{\theta}}_{ML} = \arg \max_{\hat{\boldsymbol{\theta}}} \{p(y_i(t) = y_i(t) | \hat{\boldsymbol{\theta}})\}. \quad (1.3)$$

Cependant, la solution de cette maximisation présente une forte complexité de calcul, ce qui nous mène à exploiter une technique itérative, notamment l' "Expectation-Maximization" technique.

1.2 Technique expectation-maximization

L'algorithme expectation-maximization (EM) est utilisé dans plusieurs domaines, notamment, la génétique, l'économie, et les études sociologiques ainsi que dans les domaines du traitement du signal, comme la construction des images tomographiques par approche de maximum de vraisemblance, et formation de modèles de Markov cachés en reconnaissance de la parole. L'avantage de cette technique est de résoudre le problème de manque d'informations sur les données émises, d'une manière itérative, en se basant sur des données introduites au préalable (initialisation), sans passer par des dérivations et des maximisations complexes.

Cette technique repose sur quatre étapes:

- Produire l'entrée initiale de l'algorithme, généralement en utilisant des séquences d'entraînement où les symboles émis sont parfaitement connus.
- La deuxième étape est l'expectation, où on calcule la moyenne statistique de la fonction de vraisemblance, par rapport à tous les symboles émis, en utilisant le résultat de l'itération qui précède.
- La troisième étape est la maximisation, dans laquelle on maximise le résultat de la deuxième étape, par rapport à toutes les composantes du vecteur d'inconnus θ .
- La dernière étape est l'évaluation de la fonction de vraisemblance, et comparer sa progression par rapport à la précision souhaitée.

1.3 Limites de performance de l'estimateur: la Borne de Cramér-Rao

Considérons n'importe quelle méthode d'estimation de τ et notons par $\hat{\tau}$ l'estimé correspondant. Vu que $\hat{\tau}$ dépend de l'observation y , différentes observations engendrent différents estimés. Dans ce cas $\hat{\tau}$ est une variable aléatoire dont la moyenne peut coïncider avec les vraies valeurs de τ . Dans ce cas, l'estimateur est dit non biaisé. Cette propriété est un caractère d'évaluation des performances d'estimation puisque, en moyenne, l'estimateur fournit la vraie valeur du paramètre. Cependant, l'erreur d'estimation $\hat{\tau} - \tau$ est aussi une mesure importante, d'où la nécessité de minimiser cette erreur, ou encore sa variance. Alors quand est-ce qu'on peut dire que l'erreur d'estimation est acceptable?

Dans ce contexte, la borne de Cramér-Rao est une limite théorique qui fournit une borne inférieure pour la variance de tout estimateur non-biaisé:

$$\text{var}\{\hat{\tau} - \tau\} \geq \text{CRLB}(\tau), \quad (1.4)$$

avec

$$\begin{aligned} \text{CRLB}(\tau) &= -\frac{1}{\text{E}\left\{\frac{\partial^2 \ln(\Lambda(r|\tau))}{\partial \tau^2}\right\}} \\ &= \frac{1}{\text{E}\left\{\left(\frac{\partial \ln(\Lambda(r|\tau))}{\partial \tau}\right)^2\right\}}. \end{aligned} \quad (1.5)$$

Cette borne nous permet de garantir que notre estimateur (non-biaisé) est bien l'estimateur non-biaisé à variance minimale (MVUE).

1.4 Estimateur ML du SNR

On considère un système de transmission numérique SIMO, variable dans le temps. Supposons un récepteur optimal avec une synchronisation parfaite, en temps et en fréquence. La sortie du filtre adapté à la réception peut être exprimé comme suit:

$$y_i(t_n) = h_i(t_n)a(t_n) + w_i(t_n), \quad n = 1, 2, \dots, N, \quad (1.6)$$

avec $a(t_n)$, $h_i(t_n)$ et $w_i(t_n)$ représentent respectivement le symbol émis, le coefficient du canal, et le bruit appliqué, pour la i^{eme} antenne de réception et à l' n^{eme} instant discret t_n .

En utilisant le théorème de Taylor, et après avoir appliqué les approximations et les arrangements nécessaires, on peut dégager une expansion polynomiale en fonction du temps, des coefficients du canal, comme suit:

$$h_i(t_n) = \sum_{l=0}^{L-1} c_i^{(l)} t_n^l, \quad i = 1, 2, \dots, N_r, \quad (1.7)$$

où $c_i^{(l)}$ représente le l^{eme} coefficient de l'approximation polynomiale du coefficient du canal $h_i(t_n)$, pour la i^{eme} antenne parmi les N_r antennes de réception.

Notre estimateur peut être appliqué dans le cas assisté par signaux pilotes (DA) ainsi que dans le scénario autodidacte de données inconnues (NDA).

1.4.1 Estimateur DA

Dans ce scénario, notre modèle peut être formulé comme suit:

$$\mathbf{y}_{i,\text{DA}}^{(k)} = \mathbf{A}_k \mathbf{T}' \mathbf{c}_{i,k} + \mathbf{w}_{i,k} = \mathbf{\Phi}_k \mathbf{c}_{i,k} + \mathbf{w}_{i,k}, \quad (1.8)$$

où $\Phi_k = \mathbf{A}_k \mathbf{T}'$ est une matrice de taille $(\bar{N}_{\text{DA}} \times L)$, avec L est l'ordre d'approximation polynomiale, \bar{N}_{DA} est la taille de la k^{eme} fenêtre d'approximation locale, pour le scénario DA, \mathbf{A}_k est la matrice contenant les symbols émis et \mathbf{T}' est une matrice de Vandermonde contenant les instants discrets t_n .

Après des dérivations directes, on peut dégager les résultats d'estimation des coefficients d'approximations du canal ainsi que de la variance du bruit dans le cas DA comme suit:

$$\hat{\mathbf{c}}_{k,\text{DA}} = (\mathbf{B}_k^H \mathbf{B}_k)^{-1} \mathbf{B}_k^H \mathbf{y}_{\text{DA}}^{(k)}, \quad (1.9)$$

$$\hat{\sigma}_{k,\text{DA}}^2 = \frac{1}{2\bar{N}_{\text{DA}}N_r} [\mathbf{y}_{\text{DA}}^{(k)} - \mathbf{B}_k \hat{\mathbf{c}}_{k,\text{DA}}]^H [\mathbf{y}_{\text{DA}}^{(k)} - \mathbf{B}_k \hat{\mathbf{c}}_{k,\text{DA}}], \quad (1.10)$$

avec \mathbf{B}_k est une matrice diagonale par blocs contenant les matrices Φ_k . Ainsi on obtient l'expression du MLE du SNR:

$$\hat{\rho}_{i,\text{DA}} = \frac{\hat{\mathbf{h}}_{i,\text{DA}}^H \hat{\mathbf{h}}_{i,\text{DA}}}{N(2\hat{\sigma}_{i,\text{DA}}^2)}, \quad (1.11)$$

avec $\hat{\mathbf{h}}_{i,\text{DA}} = [\hat{\mathbf{h}}_{i,\text{DA}}^{(1)}, \hat{\mathbf{h}}_{i,\text{DA}}^{(2)}, \dots, \hat{\mathbf{h}}_{i,\text{DA}}^{(N/\bar{N}_{\text{DA}})}]^T$, et $\hat{\mathbf{c}}_{i,\text{DA}}^{(k)}$, où N est la taille de la fenêtre d'observation.

On montre que cet estimateur DA du SNR est biaisé. Un estimateur non-biaisé peut être obtenu comme suit:

$$\hat{\rho}_{i,\text{DA}}^{\text{UB}} = \frac{N_r N (1 - \epsilon) - 1}{N_r N} \hat{\rho}_{i,\text{DA}} - \frac{\epsilon}{2}, \quad (1.12)$$

avec $\epsilon = L/\bar{N}_{\text{DA}}$. Après l'élimination du biais, l'MSE de notre estimateur non-biaisé tend vers la borne théorique suivante:

$$\text{MSE}\{\hat{\rho}_{i,\text{DA}}^{\text{UB}}\} \rightarrow \frac{\rho_i}{N} \left(2 + \frac{\rho_i}{N_r} \right). \quad (1.13)$$

On montre que cette borne est la borne de Cramér-Rao.

1.4.2 Estimateur NDA

Pour le scénario NDA, où les symboles émis sont inconnus pour le récepteur, on définit le modèle suivant:

$$\mathbf{y}_k(n) = a_k(n)\mathbf{C}_k\mathbf{t}(n) + \mathbf{w}_k(n), \quad (1.14)$$

avec $\mathbf{y}_k(n) = [y_{1,k}(n), y_{2,k}(n), \dots, y_{N_r,k}(n)]^T$, $a_k(n)$ est le symbole transmis correspondant, $\mathbf{C}_k = [\mathbf{c}_{1,k}, \mathbf{c}_{2,k}, \dots, \mathbf{c}_{N_r,k}]^T$ et $\mathbf{w}_k(n) = [w_{1,k}(n), w_{2,k}(n), \dots, w_{N_r,k}(n)]^T$. Dans ce scénario on a recours à la technique EM. La première étape est validée en appliquant l'estimateur DA décrit dans la section précédente. La deuxième étape est décrite comme suit:

$$Q\left(\boldsymbol{\theta}_k | \hat{\boldsymbol{\theta}}_k^{(q-1)}\right) = -\bar{N}_{\text{NDA}}N_r \ln(2\pi\sigma^2) - \frac{1}{2\sigma^2} \sum_{i=1}^{N_r} \left(M_{2,k}^{(i)} + \sum_{n=1}^{\bar{N}_{\text{NDA}}} \alpha_{n,k}^{(q-1)} |\mathbf{c}_{i,k}^T \mathbf{t}(n)|^2 - 2\beta_{i,n,k}^{(q-1)}(\mathbf{c}_{i,k}) \right), \quad (1.15)$$

avec $M_{2,k}^{(i)} = E\{|y_{i,k}(n)|^2\}$ est le moment de second ordre des échantillons à la réception pour la i^{eme} antenne de réception, et:

$$\begin{aligned} \alpha_{n,k}^{(q-1)} &= E_{a_m} \left\{ |a_m|^2 \middle| \hat{\boldsymbol{\theta}}_k^{(q-1)}, \mathbf{y}_k(n) \right\} \\ &= \sum_{m=1}^M P_{m,n,k}^{(q-1)} |a_m|^2, \end{aligned} \quad (1.16)$$

$$\begin{aligned} \beta_{i,n,k}^{(q-1)}(\mathbf{c}_{i,k}) &= E_{a_m} \left\{ \Re\{y_{i,k}^*(n)a_m \mathbf{t}^T(n)\mathbf{c}_{i,k}\} \middle| \hat{\boldsymbol{\theta}}_k^{(q-1)}, \mathbf{y}_k(n) \right\} \\ &= \sum_{m=1}^M P_{m,n,k}^{(q-1)} \Re\{y_{i,k}^*(n)a_m \mathbf{t}^T(n)\mathbf{c}_{i,k}\}. \end{aligned} \quad (1.17)$$

$P_{m,n,k}^{(q-1)} = P\left(a_m | \mathbf{y}_k(n); \hat{\boldsymbol{\theta}}_k^{(q-1)}\right)$ est la probabilité à *posteriori* de a_m à l'itération $(q-1)$ qui est calculée en utilisant la formule de Bayes comme suit:

$$P_{m,n,k}^{(q-1)} = \frac{P[a_m]P\left(\mathbf{y}_k(n) | a_m; \hat{\boldsymbol{\theta}}_k^{(q-1)}\right)}{P\left(\mathbf{y}_k(n); \hat{\boldsymbol{\theta}}_k^{(q-1)}\right)}. \quad (1.18)$$

Puisque les symboles transmis sont equiprobables, nous avons $P[a_m] = 1/M$, et par la suite:

$$P\left(\mathbf{y}_k(n); \hat{\boldsymbol{\theta}}_k^{(q-1)}\right) = \frac{1}{M} \sum_{m=1}^M P\left(\mathbf{y}_k(n) | a_m; \hat{\boldsymbol{\theta}}_k^{(q-1)}\right). \quad (1.19)$$

Le résultat de l'étape de maximisation est présenté comme suit:

$$\hat{\mathbf{c}}_{i,k}^{(q)} = \left(\sum_{n=1}^{\bar{N}_{\text{NDA}}} \mathbf{t}(n) \mathbf{t}^T(n) \right)^{-1} \left(\sum_{n=1}^{\bar{N}_{\text{NDA}}} \lambda_{i,n,k}^{(q-1)} \mathbf{t}(n) \right), \quad (1.20)$$

avec:

$$\begin{aligned} \lambda_{i,n,k}^{(q-1)} &= \underbrace{\left(\sum_{m=1}^M P_{m,n,k}^{(q-1)} a_m \right)^*}_{\hat{a}_k^{(q-1)}(n)} y_{i,k}(n), \\ &= \hat{a}_k^{(q-1)}(n)^* y_{i,k}(n). \end{aligned} \quad (1.21)$$

L'estimé de la variance du bruit est obtenu comme suit:

$$2\hat{\sigma}_k^{(q)} = \frac{\sum_{i=1}^{N_r} \left(M_{2,k}^{(i)} + \eta_{i,k}^{(q-1)} \right)}{\bar{N}_{\text{NDA}} N_r}, \quad (1.22)$$

avec:

$$\begin{aligned} \eta_{i,k}^{(q-1)} &= \sum_{n=1}^{\bar{N}_{\text{NDA}}} \left[\mathbf{t}^T(n) \left(\hat{\mathbf{c}}_{i,k}^{(q-1)} \right)^* \left(\hat{\mathbf{c}}_{i,k}^{(q-1)} \right)^T \mathbf{t}(n) + \alpha_{n,k}^{(q-1)} - 2\beta_{i,n,k}^{(q-1)} \left(\hat{\mathbf{c}}_{i,k}^{(q-1)} \right) \right] \\ &= \sum_{n=1}^{\bar{N}_{\text{NDA}}} \left[\left| \mathbf{t}^T(n) \hat{\mathbf{c}}_{i,k}^{(q-1)} \right|^2 + \alpha_{n,k}^{(q-1)} - 2\beta_{i,n,k}^{(q-1)} \left(\hat{\mathbf{c}}_{i,k}^{(q-1)} \right) \right]. \end{aligned} \quad (1.23)$$

Cet estimé local de la variance du bruit est moyenné ensuite sur les fenêtres d'approximation locales, pour obtenir un estimé plus fin qui correspond à la totalité de la fenêtre d'observation de taille N :

$$\hat{\sigma}_{\text{NDA}}^2 = \frac{\bar{N}_{\text{NDA}}}{N} \sum_{k=1}^{N/\bar{N}_{\text{NDA}}} \hat{\sigma}_{k,\text{NDA}}^2. \quad (1.24)$$

Finalement, on obtient le MLE du SNR pour le scénario NDA comme suit:

$$\hat{\rho}_{i,\text{NDA}} = \frac{\sum_{k=1}^{N/\bar{N}_{\text{NDA}}} \sum_{n=1}^{\bar{N}_{\text{NDA}}} |\mathbf{t}^T(n) \hat{\mathbf{c}}_{i,\text{NDA}}^{(k)}|^2}{N (2\hat{\sigma}_{\text{NDA}}^2)}. \quad (1.25)$$

Contents

Acknowledgements	i
Abstract	ii
1 Résumé	iv
1.1 Estimateur à maximum de vraisemblance	v
1.2 Technique expectation-maximization	vii
1.3 Limites de performance de l'estimateur: la Borne de Cramér-Rao	viii
1.4 Estimateur ML du SNR	ix
1.4.1 Estimateur DA	ix
1.4.2 Estimateur NDA	xi
List of figures	xvii
Introduction	1
2 Signal parameter estimation	5
2.1 Estimation	5

2.2	Maximum Likelihood Estimation	6
2.3	The EM algorithm	7
2.4	Cramér Rao Lower Bound (CRLB)	8
3	Derivation of the ML SNR Estimators	9
3.1	System Model	9
3.2	Derivation of the DA ML SNR Estimator and the CRLB	12
3.2.1	Formulation of the DA ML SNR Estimator	12
3.2.2	Derivation of the exact bias and variance for the DA ML estimator .	16
3.2.3	Derivation of the DA CRLB	19
3.3	Formulation of the new NDA ML SNR estimator	20
3.3.1	New NDA ML SNR Estimator	20
3.3.2	The previously presented work (<i>WL</i>) and its SIMO extension	29
4	Simulation Results	31
4.1	Overflow problem correction	32
4.2	Simulation results	34
	Conclusion	47
	Appendix A	48
	Appendix B	50

List of Figures

4.1	True vs. estimated channel envelope with overflow (a) and corrected-overflow (b), for $f_D T_s = 3, 5 \cdot 10^{-2}$, $N = 112$, $\bar{N}_{\text{DA}} = 28$, $\bar{N}_{\text{NDA}} = 14$ and $(L = 4)$	34
4.2	NMSE for the “ <i>pilot-only DA</i> ”, “ <i>completely DA</i> ”, “ <i>hybrid NDA</i> ” and “ <i>completely NDA</i> ” estimators vs. the average SNR γ , with $N_r = 2$, $N = 112$, $\bar{N}_{\text{DA}} = 112$, $\bar{N}_{\text{NDA}} = N/2 = 56$, $f_D T_s = 7 \cdot 10^{-3}$ and $L = 4$	35
4.3	True vs. estimated channel magnitude for the EM-based algorithm when initialized (a) arbitrarily with ones, and (b) appropriately with the “ <i>pilot-only DA</i> ” estimates, for $f_D T_s = 3.5 \cdot 10^{-2}$, $N = 112$, $\bar{N}_{\text{DA}} = 28$, $\bar{N}_{\text{NDA}} = 14$, and $L = 4$	36
4.4	NMSE for the “ <i>static ML</i> ” and the “ <i>hybrid NDA</i> ” EM-based estimator ($L = 4$) vs. the average SNR γ , for different values of $f_D T_s$ (a) $f_D T_s = 3, 5 \cdot 10^{-4}$ (b) $f_D T_s = 3, 5 \cdot 10^{-3}$ (c) $f_D T_s = 3, 5 \cdot 10^{-2}$, with $N = 112$ and $N_r = 2$	37
4.5	NMSE for the “ <i>WL</i> ”, the “ <i>completely DA</i> ”, the “ <i>completely NDA</i> ” and the <i>hybrid NDA</i> EM-based estimator ($L = 4$) and the NCRLB_{DA} vs. the average SNR γ , for SISO time-varying channels with $f_D T_s = 7 \cdot 10^{-3}$, $N = \bar{N}_{\text{DA}} = 112$, and $\bar{N}_{\text{NDA}} = 56$	39

4.6	NMSE for WGL-SIMO, the “ <i>completely DA</i> ”, the “ <i>completely NDA</i> ” and the <i>hybrid NDA</i> estimators vs. the average SNR γ , for $f_D T_s = 7 \cdot 10^{-3}$, $N = 112$, $\bar{N}_{DA} = 112$, and $\bar{N}_{NDA} = 56$, $L = 4$	40
4.7	NMSE for the unbiased version of the <i>completely DA</i> and the <i>hybrid estimators</i> vs. the average SNR, for different numbers of receiving antenna elements with: $N = 112$, $\bar{N}_{DA} = 112$, $\bar{N}_{NDA} = 56$, $f_D T_s = 7 \cdot 10^{-3}$, and $L = 4$	42
4.8	NMSE for the the “ <i>hybrid NDA</i> ” EM-based and the “ <i>completely DA</i> ” unbiased estimators vs. the average SNR with $N = 112$ and $N_r = 2$ for: (a) $f_D T_s = 7 \cdot 10^{-3}$, $\bar{N}_{DA} = 112$, $\bar{N}_{NDA} = 56$, (b) $f_D T_s = 2 \cdot 10^{-2}$, $\bar{N}_{DA} = 28$, $\bar{N}_{NDA} = 28$, (c) $f_D T_s = 7 \cdot 10^{-3}$, $\bar{N}_{DA} = 28$, $\bar{N}_{NDA} = 14$ and (d) $f_D T_s = 7 \cdot 10^{-3}$, $\bar{N}_{DA} = 14$, $\bar{N}_{NDA} = 7$	44
4.9	NMSE for the unbiased “ <i>hybrid NDA</i> ” and <i>completely DA</i> estimators vs. the average SNR, for different constellations types and orders with $N = \bar{N}_{DA} = 112$, $\bar{N}_{NDA} = 56$, $N_r = 2$ and $f_D T_s = 7 \cdot 10^{-3}$, and $L = 4$	46

Introduction

Over the recent years, there has been an increasing demand for the *a priori* knowledge of the propagation environment conditions, fuelled by an increasing thirst for taking advantage of any optimization opportunity that would enhance the system capacity. In essence, almost all the necessary information about these propagation conditions can be captured by estimating various channel parameters. In particular, the SNR is considered as a key parameter whose *a priori* knowledge can be exploited at both the receiver and the transmitter (through feedback), in order to reach the desired enhanced/optimal performance using various adaptive schemes. For instance, the information about the SNR is required in all power control strategies, adaptive coding and modulation schemes, turbo decoding as well as to provide the channel quality information for handoff schemes [1-3], just to name a few. Roughly speaking, SNR estimators can be broadly divided into two major categories: i) data-aided (DA) techniques in which the estimation process relies on a perfectly known (pilot) transmitted sequence, and ii) non-data-aided (NDA) techniques where the estimation process is applied blindly using the received samples only.

In principle, DA approaches often provide sufficiently accurate estimates for constant or quasi-constant parameters, even using a reduced number of pilot symbols. However, in fast

changing wireless channels, they require larger pilot sequences in order to track the time variations of the unknown parameter. Indeed, in the special case of estimating the *instantaneous* SNR from pilot symbols, that are usually placed far apart in time, the DA approaches are usually unable to reflect the actual channel quality. This is because the receiver cannot accurately capture the details of the channel variations between the pilot positions. In principle, this problem can be dealt with by inserting more pilot symbols. Unfortunately, this remedy results in an excessive overhead that causes a severe loss in system capacity. To avoid doing so, NDA approaches are often considered as they are able to use both pilot and non-pilot received samples to estimate the channel coefficients. Consequently, they provide the receiver with more refined channel tracking capabilities without impinging on the whole throughput of the system.

Historically, the problem of SNR estimation was first formulated and tackled in the context of single-input single-output (SISO) systems under constant channels [4, 5]. These two early estimators, among which the well-known M2M4 technique, are moment-based ones. The M2M4 estimator in particular is based on the second- and forth-order moments. During the last decade, there has been a surge of interest in investigating this problem more intensively [6-9] and most of the presented works focused also on the NDA moment-based solutions. Indeed, a six-order moment-based estimator was proposed in [9]. Another eight-order moment-based estimator was also reported in [10]. A more general class of higher-order moment-based estimators was also introduced in [8]. Yet, in spite of enjoying a very easy implementation in real-world platforms, these NDA moment-based techniques were primarily designed for constant channels. They also require a very large number of received samples

to accurately estimate the SNR. This is in part due to the fact that they do not exploit the whole information carried by the inphase (I) and quadrature (Q) components of the received signal. Hence, I/Q-based maximum-likelihood (ML) approaches have also been recently investigated in [6] and [13], but again in the special case of constant SISO channels.

More recently, SNR estimation has been addressed under different types of diversity. In particular, considering SIMO systems (i.e., spatial diversity), a moment-based SNR estimator that exploits the fourth-order cross-moments (between the antenna elements) was proposed in [11, 12]. As far as ML SNR estimation is concerned, spatial diversity has also been investigated in [14, 15] under SIMO and MIMO systems, respectively. However, most of the works that have been conducted on the topic of SNR estimation, including all the aforementioned techniques, focused only on constant or slowly time-varying channels, thereby suffering from severely degraded performance under fast time-varying channels. Yet, current and future generation systems such as LTE, LTE-Advanced and beyond are expected to support reliable communications at velocities that can reach 500 Km/h [17]. In these situations, classical assumptions where the channel is considered as constant during the observation window do not hold, and hence there is a need to explicitly incorporate the channel time-variations in the estimation process. To date and to the best of our knowledge, the only work that has so far considered ML SNR estimation under time-varying channels is [18], but again in the special case of traditional SISO systems. As far as SIMO configurations are concerned, time-varying channels were considered in [19] where a least-square (LS)-based approach was developed, relying on detected data in a decision-directed (DD) scheme.

Motivated by all these facts, we tackle in this thesis the problem of ML *instantaneous* SNR

estimation over time-varying SIMO channels, both for the DA and NDA schemes. Our proposed method is based on a piece-wise polynomial-in-time approximation for the channel process with few unknown coefficients. In the DA scenario where the receiver has access to a pilot sequence from which the SNR is to be obtained, the ML estimator is derived in closed-form. Whereas, in the NDA case where the transmitted data is unknown or partially available, the corresponding likelihood function is very complicated and its analytical maximization is mathematically intractable. Therefore, we resort to a more elaborate solution using the EM concept, and we develop thereby an iterative technique that is able to converge to the *exact* NDA ML estimates within very few iterations (i.e., in the range of 10). Simulation results show the distinct performance advantage offered by exploiting the spatial diversity in terms of instantaneous SNR estimation.

Chapter 2

Signal parameter estimation

2.1 Estimation

The problem of parameter estimation is a common problem that is widely faced in many areas such as Radar, image analysis, communications, and much more. The problem we are faced with is estimating some parameters based on some observed samples due to the use of digital communication systems or digital computers [20]. Mathematically speaking, we observe N data points at the receiver side $\{y(1), y(2), \dots, y(N)\}$ which sampled from an unknown probability density function $p_Y(y; \boldsymbol{\theta})$ parameterized by an unknown parameter vector $\boldsymbol{\theta}$, which is the parameter vector of interest. Unfortunately, we do not really get to see the distribution of the received sample Y . We only get that sample, Y , which we then use to estimate our parameter $\boldsymbol{\theta}$. As a result of that, our estimator will not give us the exact value of $\boldsymbol{\theta}$, but an estimated version of it. Our estimator will depend highly through some

function of the received sample Y as:

$$\hat{\boldsymbol{\theta}} = f\{y(1), y(2), \dots, y(N)\}. \quad (2.1)$$

This estimator might be used to estimate the carrier frequency, channel phase, signal power, noise power, SNR, etc. Since the received data are random, we can describe its behavior according to its PDF function $p(y(1), y(2), \dots, y(N); \boldsymbol{\theta})$. The operator ';' is used to indicate that the distribution of PDF is parameterized by the parameter $\boldsymbol{\theta}$.

2.2 Maximum Likelihood Estimation

The ML estimators are known to be the most accurate techniques, since unlike other existing estimators, they rely the estimation procedure on the whole information carried by the inphase and quadrature (I/Q) components. In order to obtain the ML estimates, we must derive the likelihood function, which is a function of the parameters of a statistical model given the observation data, given by $p(y(1), y(2), \dots, y(N); \boldsymbol{\theta})$. The maximum likelihood solution selects values for the model parameters that give a distribution which gives the observed data the highest probability. Therefore, to obtain the ML estimates of the desired parameter, we go through maximizing the likelihood function. Since it is a monotonic function, it will be more convenient to maximize the Log likelihood function instead. But since in real scenarios we do not have access to the transmitted data, we are often faced against a complicated Log likelihood function whose maximization is mathematically intractable. Therefore, we must resort to a more relevant technique, namely the Expectation-Maximization technique which is described in the next section.

2.3 The EM algorithm

The EM algorithm was invented and implemented by several researchers until Dempster [21] collected their ideas together, assured convergence, and stated the term “EM algorithm”, which has been used since then. One of the main application areas of the EM algorithm is estimating parameters of mixture distribution which is the aim in this research. The EM algorithm has broad areas of applications some of which is in genetics, econometric, clinical, and sociological studies. It is also used in signal processing areas like Maximum Likelihood tomographic image reconstruction, training of hidden Markov models in speech recognition. The advent of the EM algorithm has come to solving the problem of latent (unobserved) variables which MLE could not afford. If we introduce a joint distribution over both the observed and hidden variables, then the corresponding distribution (the distribution of the observed variables alone) is given by marginalization. This would help putting complex distributions over observed variables to be in a more tractable form of distribution formed by both observed and latent variables. Therefore, the EM algorithm would be the method of choice when direct maximum likelihood (ML) parameter estimation is not possible without the knowledge of the latent variables. The goal of the EM algorithm is to find the Maximum Likelihood (ML) solutions for models which have latent variables. The main objective in this thesis, is to exploit this concept in order to derive the ML solution for the SNR.

The EM algorithm can be divided into 4 steps:

- First, we begin by providing the initial input $\hat{\theta}^{(0)}$, then calculate the initial value of the Log likelihood function.

- Then, the second step is the Expectation step or the E step, in which we calculate the expectation of the Log likelihood function with respect to all possible transmitted data using the result of the estimated parameter vector obtained in the previous iteration.
- The third step is then the Maximization step or the M step where we maximize the output of the E step, with respect to all elementary components of the parameter vector θ .
- Finally, in the final step, we evaluate the Log likelihood function, and compare its progression to the desired precision. If the precision has not been achieved, we go back to step number 2 and iterate once again and we repeat the same procedure until we achieve the precision condition.

2.4 Cramér Rao Lower Bound (CRLB)

Generally, the estimators performances are evaluated in terms of variance. In fact, we need to find the minimum variance estimator we can obtain. But unfortunately, this estimator does not always exist, and if it does, sometimes it is not easy to find. One way of finding it is using the Cramér Rao Lower Bound (CRLB). Finding a lower bound on the variance of an unbiased estimator will be extremely important in practice. This will serve as a benchmark in comparing the performance of an estimator. CRLB allows us to assure that an estimator is the minimum variance unbiased estimator (MVUE), which will be the case when the estimator attains the CRLB for all values of the unknown parameter.

Chapter 3

Derivation of the ML SNR Estimators

3.1 System Model

Consider a digital communication SIMO system transmitting over a frequency-flat time-varying channel. Assuming an ideal receiver with perfect time and frequency synchronization, and after matched filtering, the sampled baseband received signal over the i^{th} antenna element can be expressed as:

$$y_i(t_n) = h_i(t_n)a(t_n) + w_i(t_n), \quad n = 1, 2, \dots, N \quad (3.1)$$

where $\{t_n = nT_s\}_{n=1}^N$ is the n^{th} discrete-time instant, T_s is the sampling period, and N is the size of the observation window. We denote by $a(t_n)$ the linearly-modulated (M-PSK, M-PAM or M-QAM) transmitted symbol, by $y_i(t_n)$ the corresponding received sample, and by $h_i(t_n)$ the time-varying *complex* channel gain, over the i^{th} antenna branch. The noise components, $w_i(t_n)$, assumed to be temporally white and uncorrelated between antenna elements, are realizations of a zero-mean complex circular Gaussian process, with independent

real and imaginary parts, each of variance σ^2 (i.e., with overall noise power $2\sigma^2$). We assume that the same noise power is experienced over all the antenna branches (*uniform* noise). As mentioned previously, most of the classical techniques are based on the assumption that the channels are constant during the observation period, i.e., $h_i(t_n) = h_i$ for $n = 1, 2, \dots, N$. But since in most real-world situations this assumption does not hold, we can track the channel evolution using a polynomial-in-time approximation model [22]. In fact, using Taylor's theorem, the time variations of the channel coefficients can be locally tracked through a polynomial-in-time expansion of order $(L - 1)$ as follows:

$$h_i(t_n) = \sum_{l=0}^{L-1} c_i^{(l)} t_n^l + R_L^{(i)}(n), \quad i = 1, 2, \dots, N_r \quad (3.2)$$

where $c_i^{(l)}$ is the l^{th} coefficient of the channel polynomial approximation over the i^{th} branch among N_r receiving antennae and $\{t_n = nT_s\}_{n=1}^N$. The term $R_L^{(i)}(n)$ refers to the remainder of the Taylor's series expansion. This remainder can be driven to zero under mild conditions, such as i) a sufficiently high approximation order $(L - 1)$, or ii) a sufficiently small ratio $\bar{N}F_d/F_s$, where $F_s = 1/T_s$ is the sampling rate, F_d is the maximum Doppler frequency shift, and \bar{N} is the size of the local approximation window. Choosing a high approximation order (first condition) may result in numerical instabilities due to badly conditioned matrices (depending on the value of the sampling rate). The second condition, however, can be easily fulfilled by choosing small-size local-approximation windows by appropriately selecting \bar{N} . By doing so, the remainder $R_L^{(i)}(n)$ can be neglected thereby yielding the following approximation:

$$h_i(t_n) = \sum_{l=0}^{L-1} c_i^{(l)} t_n^l, \quad i = 1, 2, \dots, N_r. \quad (3.3)$$

Our goal in this thesis can be basically formulated as follows: given all the received samples $\{y_i(n)\}_{n=1}^N$, for $i = 1, 2, \dots, N_r$, and the statistical noise model, we will estimate (continuously) the *instantaneous* SNR which can be expressed as:

$$\rho_i = \frac{\mathbb{E}\{|h_i(t_n)|^2|a(t_n)|^2\}}{2\sigma^2} = \frac{|h_i(t_n)|^2\mathbb{E}\{|a(t_n)|^2\}}{2\sigma^2}. \quad (3.4)$$

But since we further assume that the transmit energy is normalized¹ to one, i.e., $\mathbb{E}\{|a(t_n)|^2\} = 1$, and taking into account the polynomial expansion of $h_i(t_n)$ in (3.3), the *instantaneous* SNRs to be estimated reduce simply to:

$$\rho_i = \frac{\sum_{n=1}^N \left| \sum_{l=0}^{L-1} c_i^{(l)} t_n^l \right|^2}{N(2\sigma^2)}, i = 1, 2, \dots, N_r. \quad (3.5)$$

Note that we do not make any further assumption about the channel coefficients rather than being unknown but deterministic. Of course, they might be random in practice but we are not willing to assume any *a priori* knowledge about the channel statistical model. The motivations behind this choice are twofold: i) the statistical models are after all theoretical ones and may not reflect the true behaviour of real-world channels and ii) the fading conditions (for instance the presence of a line-of-sight component or not) might change in real time as users move from one location to another. In light of the above reasons, the new estimator is hence well geared toward any type of fading, a quite precious degree of freedom in practice. Besides, the main advantage of local tracking is its ability to capture the unpredictable time variations of the channel gains using very few coefficients. Thus, we split up the entire observation window (of size N) into multiple local *approximation* windows of size \bar{N} (where

¹Note that normalization is assumed here only for the sake of simplicity. If the transmit energy, P , is not unitary, then it can be easily incorporated as an unknown scaling factor into the channel coefficients by estimating $\tilde{h}_i(t_n) = Ph_i(t_n)$ instead of $h_i(t_n)$.

N is an integer multiple of \bar{N}). Then, after acquiring all the locally estimated polynomial coefficients $\{\hat{c}_{i,k}^{(l)}\}_{k=1}^{N/\bar{N}}$, where k is the index of each local approximation window, and after averaging the local estimates² of the single-sided noise power, $\{\hat{\sigma}_k^2\}_{k=1}^{N/\bar{N}}$, the estimated SNRs are ultimately obtained as:

$$\hat{\rho}_i = \frac{\sum_{k=1}^{N/\bar{N}} \sum_{n=1}^{\bar{N}} \left| \sum_{l=0}^{L-1} \hat{c}_{i,k}^{(l)} t_n^l \right|^2}{N \left(\frac{\bar{N}}{N} \sum_{k=1}^{N/\bar{N}} 2\hat{\sigma}_k^2 \right)}, \quad i = 1, 2, \dots, N_r. \quad (3.6)$$

3.2 Derivation of the DA ML SNR Estimator and the CRLB

In this section, we begin by deriving in closed-form expression the DA ML estimator for the SNR over each antenna element. Then, we will derive its bias revealing thereby that the derived estimator is actually biased due to the neglected remainder of the Taylor's series. This will afterward allow us to obtain an unbiased version of the DA estimator by removing this bias during the estimation process. Finally, we will derive the closed-form expressions for the corresponding variance and CRLB. Recall that in the DA case the transmitted sequence, from which the SNRs will be estimated, is assumed to be perfectly known to the receiver.

3.2.1 Formulation of the DA ML SNR Estimator

In most real-world applications, some known pilot symbols are usually inserted to perform different synchronization tasks. The DA ML estimator can thus rely on these pilot sequences to estimate the *instantaneous* SNR or at least to give a head start for an iterative algorithm,

²These are indeed multiple estimates of the same constant but unknown parameter σ^2 .

as will be derived in the next section, by providing a good initial guess about the unknown parameters. Thus, in the current scenario, only the received samples corresponding to pilot positions are used during the estimation process. Assume, therefore, that N' such known symbols are periodically transmitted every $T'_s = N_p T_s$ where $N_p \geq 1$ is an integer quantifying the normalized (by T_s) time period between any two consecutive pilot positions. Here, we denote the size of the local approximation windows as \bar{N}_{DA} (later in this chapter, we shall use $\bar{N} = \bar{N}_{\text{NDA}}$ for the NDA case). To begin with, we consider each antenna element, i , and gather all the corresponding received (pilot) samples within each approximation window, k , in a column vector $\mathbf{y}_{i,\text{DA}}^{(k)} = [y_i^{(k)}(t'_1), y_i^{(k)}(t'_2), \dots, y_i^{(k)}(t'_{\bar{N}_{\text{DA}}})]^T$, where $t'_n = n T'_s$ for $n = 1, 2, \dots, \bar{N}_{\text{DA}}$. Moreover, the channel coefficients at each pilot position, t'_n , are obtained from (3.3) as follows:

$$h_{i,k}(t'_n) = \sum_{l=0}^{L-1} c_{i,k}^{(l)} t_n^l, \quad i = 1, 2, \dots, N_r. \quad (3.7)$$

For mathematical convenience, we also define the following vectors:

$$\begin{aligned} \mathbf{h}_{i,k} &= [h_{i,k}(t'_1), h_{i,k}(t'_2), \dots, h_{i,k}(t'_{\bar{N}_{\text{DA}}})]^T \\ \mathbf{w}_{i,k} &= [w_{i,k}(t'_1), w_{i,k}(t'_2), \dots, w_{i,k}(t'_{\bar{N}_{\text{DA}}})]^T \\ \mathbf{c}_{i,k} &= [c_{i,k}^{(0)}, c_{i,k}^{(1)}, \dots, c_{i,k}^{(L-1)}]^T \end{aligned} \quad (3.8)$$

where, over the i^{th} antenna branch and the local approximation window k , $\mathbf{h}_{i,k}$ contains the time-varying *complex* channel gains, $\mathbf{c}_{i,k}$ is a vector of the corresponding polynomial coefficients and $\mathbf{w}_{i,k}$ is the noise vector. Then, using (3.7), we can rewrite the channel approximation model in a more compact form as follows:

$$\mathbf{h}_{i,k} = \mathbf{T}' \mathbf{c}_{i,k}, \quad i = 1, 2, \dots, N_r \quad (3.9)$$

where:

$$\mathbf{T}' = \begin{pmatrix} 1 & t'_1 & \cdots & t'^{L-1}_1 \\ 1 & t'_2 & \cdots & t'^{L-1}_2 \\ \vdots & \vdots & \ddots & \vdots \\ 1 & t'_{\bar{N}_{\text{DA}}} & \cdots & t'^{L-1}_{\bar{N}_{\text{DA}}} \end{pmatrix}. \quad (3.10)$$

Note that \mathbf{T}' is a Vandermonde matrix with linearly independent columns. Consequently, it is a full-rank matrix meaning that the pseudo-inverse that will appear in the sequel is always well defined.

Let \mathbf{A}_k be the $(\bar{N}_{\text{DA}} \times \bar{N}_{\text{DA}})$ diagonal matrix that contains all the known transmitted symbols during the k^{th} approximation window:

$$\mathbf{A}_k = \begin{pmatrix} a_k(t'_1) & 0 & \cdots & 0 \\ 0 & a_k(t'_2) & \cdots & 0 \\ \vdots & \vdots & \ddots & \vdots \\ 0 & 0 & \cdots & a_k(t'_{\bar{N}_{\text{DA}}}) \end{pmatrix}. \quad (3.11)$$

Using (3.8) and (3.11), we can rewrite the corresponding received samples (over each antenna element i) in a \bar{N}_{DA} -dimensional column vector as follows:

$$\mathbf{y}_{i,\text{DA}}^{(k)} = \mathbf{A}_k \mathbf{T}' \mathbf{c}_{i,k} + \mathbf{w}_{i,k} = \mathbf{\Phi}_k \mathbf{c}_{i,k} + \mathbf{w}_{i,k} \quad (3.12)$$

where $\mathbf{\Phi}_k = \mathbf{A}_k \mathbf{T}'$ is a $(\bar{N}_{\text{DA}} \times L)$ matrix. We further stack all these per-antenna local observation vectors, $\{\mathbf{y}_{i,\text{DA}}^{(k)}\}_{i=1}^{N_r}$, one below another into a single vector $\mathbf{y}_{\text{DA}}^{(k)} = [\mathbf{y}_{1,\text{DA}}^{(k)T} \ \mathbf{y}_{2,\text{DA}}^{(k)T} \ \cdots \ \mathbf{y}_{N_r,\text{DA}}^{(k)T}]^T$.

In this way, all the (space-time) received samples corresponding to the k^{th} approximation window can be written in a more succinct vector/matrix form as follows:

$$\mathbf{y}_{\text{DA}}^{(k)} = \mathbf{B}_k \mathbf{c}_k + \mathbf{w}_k \quad (3.13)$$

where $\mathbf{c}_k = [\mathbf{c}_{1,k}^T \ \mathbf{c}_{2,k}^T \ \cdots \ \mathbf{c}_{N_r,k}^T]^T$ and $\mathbf{w}_k = [\mathbf{w}_{1,k}^T \ \mathbf{w}_{2,k}^T \ \cdots \ \mathbf{w}_{N_r,k}^T]^T$ are LN_r - and $\bar{N}_{\text{DA}}N_r$ -dimensional column vectors, respectively, vectorized in the same way and \mathbf{B}_k is a $(\bar{N}_{\text{DA}}N_r \times LN_r)$ block-diagonal matrix given by $\mathbf{B}_k = \text{blkdiag}\{\Phi_k, \Phi_k, \dots, \Phi_k\}$. From (3.13), the probability density function (pdf) of the locally observed vectors, $\mathbf{y}_{\text{DA}}^{(k)}$, conditioned on \mathbf{B}_k and parameterized by $\boldsymbol{\theta}_k = [\mathbf{c}_k^T, \sigma^2]^T$ (a vector that contains all the unknown parameters over the k^{th} approximation window) is given by:

$$p(\mathbf{y}_{\text{DA}}^{(k)}; \boldsymbol{\theta}_k | \mathbf{B}_k) = \frac{1}{(2\pi\sigma^2)^{\bar{N}_{\text{DA}}N_r}} \exp \left\{ -\frac{1}{2\sigma^2} [\mathbf{y}_{\text{DA}}^{(k)} - \mathbf{B}_k \mathbf{c}_k]^H [\mathbf{y}_{\text{DA}}^{(k)} - \mathbf{B}_k \mathbf{c}_k] \right\}. \quad (3.14)$$

The natural logarithm of (3.14) yields the so-called DA log-likelihood function, $L_{\text{DA}}(\boldsymbol{\theta}_k) = \ln(p(\mathbf{y}_{\text{DA}}^{(k)}; \boldsymbol{\theta}_k | \mathbf{B}_k))$, as follows:

$$L_{\text{DA}}(\boldsymbol{\theta}_k) = -\bar{N}_{\text{DA}}N_r \ln(2\pi) - \bar{N}_{\text{DA}}N_r \ln(\sigma^2) - \frac{1}{2\sigma^2} [\mathbf{y}_{\text{DA}}^{(k)} - \mathbf{B}_k \mathbf{c}_k]^H [\mathbf{y}_{\text{DA}}^{(k)} - \mathbf{B}_k \mathbf{c}_k]. \quad (3.15)$$

By differentiating (3.15) with respect to the vector \mathbf{c}_k and setting it to zero, we obtain the ML estimate of the local polynomial coefficients over all the receiving antenna branches as follows:

$$\hat{\mathbf{c}}_{k,\text{DA}} = (\mathbf{B}_k^H \mathbf{B}_k)^{-1} \mathbf{B}_k^H \mathbf{y}_{\text{DA}}^{(k)} \quad (3.16)$$

where \mathbf{T}' and \mathbf{A}_k are known matrices, hence the matrix \mathbf{B}_k . Note also that $\mathbf{B}_k^H \mathbf{B}_k$ is a block-diagonal matrix and hence its inverse can be easily obtained by computing the inverses of its small-size diagonal blocks separately. To estimate the noise variance, we first find the partial derivative of (3.15), with respect to σ^2 . Then after setting it to zero and substituting \mathbf{c}_k by $\hat{\mathbf{c}}_{k,\text{DA}}$ obtained in (3.16), the ML estimate for the noise variance is derived as follows:

$$\hat{\sigma}_{k,\text{DA}}^2 = \frac{1}{2\bar{N}_{\text{DA}}N_r} [\mathbf{y}_{\text{DA}}^{(k)} - \mathbf{B}_k \hat{\mathbf{c}}_{k,\text{DA}}]^H [\mathbf{y}_{\text{DA}}^{(k)} - \mathbf{B}_k \hat{\mathbf{c}}_{k,\text{DA}}]. \quad (3.17)$$

Actually, combining (3.16) and (3.17), it can be further shown that:

$$\begin{aligned}\widehat{\sigma}_{k,\text{DA}}^2 &= \frac{1}{2\bar{N}_{\text{DA}}N_r} \left[\mathbf{y}_{\text{DA}}^{(k)H} (\mathbf{I} - \mathbf{P}_k) \mathbf{y}_{\text{DA}}^{(k)} \right] \\ &= \frac{1}{2\bar{N}_{\text{DA}}N_r} \left[\mathbf{y}_{\text{DA}}^{(k)H} \mathbf{P}_k^\perp \mathbf{y}_{\text{DA}}^{(k)} \right]\end{aligned}\quad (3.18)$$

in which $\mathbf{P}_k = \mathbf{B}_k (\mathbf{B}_k^H \mathbf{B}_k)^{-1} \mathbf{B}_k^H$ and $\mathbf{P}_k^\perp = \mathbf{I} - \mathbf{P}_k$ are, respectively, the projection matrices onto the column space of \mathbf{B}_k (i.e., signal subspace) and its orthogonal complement (noise subspace). In order to obtain the estimated SNRs over the entire observation window, for each antenna element i , we extract the corresponding locally estimated polynomial coefficients, $\{\widehat{\mathbf{c}}_{i,\text{DA}}^{(k)}\}_k$, from which we obtain the channel coefficients over each approximation window, $\{\widehat{\mathbf{h}}_{i,\text{DA}}^{(k)} = \mathbf{T}' \widehat{\mathbf{c}}_{i,\text{DA}}^{(k)}\}_k$. The latters are then stacked, for each antenna branch, in a single vector $\widehat{\mathbf{h}}_{i,\text{DA}} = [\widehat{\mathbf{h}}_{i,\text{DA}}^{(1)}, \widehat{\mathbf{h}}_{i,\text{DA}}^{(2)}, \dots, \widehat{\mathbf{h}}_{i,\text{DA}}^{(N/\bar{N}_{\text{DA}})}]^T$. On the other hand, the local estimates for the noise variance are averaged over all the approximation windows:

$$\widehat{\sigma}_{\text{DA}}^2 = \frac{\bar{N}_{\text{DA}}}{N} \sum_{k=1}^{N/\bar{N}_{\text{DA}}} \widehat{\sigma}_{k,\text{DA}}^2 \quad (3.19)$$

to finally obtain the DA ML SNR estimator as follows:

$$\widehat{\rho}_{i,\text{DA}} = \frac{\widehat{\mathbf{h}}_{i,\text{DA}}^H \widehat{\mathbf{h}}_{i,\text{DA}}}{N(2\widehat{\sigma}_{\text{DA}}^2)}. \quad (3.20)$$

3.2.2 Derivation of the exact bias and variance for the DA ML estimator

To improve the accuracy of the DA ML estimator, we calculate and remove its bias in order to obtain an unbiased version. After doing so, we will derive the exact expression for the variance of the obtained unbiased estimator. In fact, recall from (3.6) that the ML DA SNR

estimates are given by:

$$\hat{\rho}_{i,\text{DA}} = \frac{\sum_{k=1}^{N/\bar{N}_{\text{DA}}} \sum_{n=1}^{\bar{N}_{\text{DA}}} \left| \sum_{l=0}^{L-1} \hat{c}_{i,k}^{(l)} t_n^l \right|^2}{N \left(\frac{\bar{N}_{\text{DA}}}{N} \sum_{k=1}^{N/\bar{N}_{\text{DA}}} 2\hat{\sigma}_{k,\text{DA}}^2 \right)} \quad (3.21)$$

from which it can be shown that the estimator is a scaled noncentral F distributed random variable [23]:

$$\frac{2(N - \frac{N}{\bar{N}_{\text{DA}}}L)}{\frac{N}{\bar{N}_{\text{DA}}}L} \hat{\rho}_{i,\text{DA}} = F_{v_1, v_2}(\lambda), \quad (3.22)$$

where $F_{v_1, v_2}(\lambda)$ is the noncentral F distribution with noncentrality parameter $\lambda = 2N\rho_i$ and with degrees of freedom $v_1 = \frac{N}{\bar{N}_{\text{DA}}}L$ and $v_2 = 2N_r(N - \frac{N}{\bar{N}_{\text{DA}}}L)$. Hence, the mean and the variance of the new DA ML estimator follow immediately from the following two expressions:

$$\text{E}\{F\} = \frac{v_2(v_1 + \lambda)}{v_1(v_2 - 2)}, \quad v_2 > 2 \quad (3.23)$$

$$\text{Var}\{F\} = 2 \left(\frac{v_2}{v_1} \right)^2 \frac{(v_1 + \lambda)^2 + (v_1 + 2\lambda)(v_2 - 2)}{(v_2 - 2)^2(v_2 - 4)}, \quad v_2 > 4. \quad (3.24)$$

Indeed, using (3.22) through (3.24) and denoting $\epsilon = L/\bar{N}_{\text{DA}}$, it can be shown that:

$$\text{E}\{\hat{\rho}_{i,\text{DA}}\} = \text{E}\left\{ \frac{\epsilon}{2(1 - \epsilon)} F \right\} = \frac{N_r N}{N_r N(1 - \epsilon) - 1} \left(\rho_i + \frac{\epsilon}{2} \right) \quad (3.25)$$

and

$$\text{Var}\{\hat{\rho}_{i,\text{DA}}\} = \frac{(N_r N)^2 \left[\rho_i^2 + \rho_i \left(2N_r(1 - \epsilon) + \epsilon - \frac{2}{N} \right) + \left(\frac{N_r}{2} - \frac{1}{2N} \right) \epsilon - \left(\frac{N_r}{2} - \frac{1}{4} \right) \epsilon^2 \right]}{\left(N_r N(1 - \epsilon) - 1 \right)^2 \left(N_r N(1 - \epsilon) - 2 \right)} \quad (3.26)$$

Now, using (3.25), we can derive the exact bias for the DA estimator as follows:

$$\text{Bias}\{\hat{\rho}_{i,\text{DA}}\} = \rho_i \left(\frac{N_r N}{N_r N(1 - \epsilon) - 1} - 1 \right) + \frac{N_r N \epsilon}{2N_r N(1 - \epsilon) - 1} \neq 0 \quad (3.27)$$

which is not identically zero, meaning that the estimator is actually biased. As stated previously, this bias stems from dropping the Taylor's remainder in the channel approximation model. Yet, an unbiased version of this DA estimator (i.e., $E\{\widehat{\rho}_{i,\text{DA}}^{\text{UB}}\} = \rho_i$) can be straightforwardly obtained from (3.25) as follows:

$$\widehat{\rho}_{i,\text{DA}}^{\text{UB}} = \frac{N_r N (1 - \epsilon) - 1}{N_r N} \widehat{\rho}_{i,\text{DA}} - \frac{\epsilon}{2}. \quad (3.28)$$

Therefore, by combining (3.26) and (3.28), it follows that:

$$\text{Var}\{\widehat{\rho}_{i,\text{DA}}^{\text{UB}}\} = \frac{1}{N N_r (1 - \epsilon) - 2} \left[\rho_i^2 + \rho_i \left(2N_r (1 - \epsilon) + \epsilon - \frac{2}{N} \right) + \left(\frac{N_r}{2} - \frac{1}{2N} \right) \epsilon - \left(\frac{N_r}{2} - \frac{1}{4} \right) \epsilon^2 \right].$$

It can be verified that asymptotically³, i.e., when $N \gg 1$ and $\bar{N}_{\text{DA}} \gg L$ (or equivalently $\epsilon \ll 1$), the mean square error (or the variance) of the unbiased estimator $\text{MSE}\{\widehat{\rho}_{i,\text{DA}}^{\text{UB}}\} = E\{(\widehat{\rho}_{i,\text{DA}}^{\text{UB}} - \rho_i)^2\}$ tends to the following interesting theoretical bound:

$$\text{MSE}\{\widehat{\rho}_{i,\text{DA}}^{\text{UB}}\} \rightarrow \frac{\rho_i}{N} \left(2 + \frac{\rho_i}{N_r} \right) \quad (3.29)$$

which is nothing but the so-called CRLB that will be derived in the next subsection. Therefore, our unbiased DA ML estimator is asymptotically efficient and attains the theoretical optimal performance as will be validated by computer simulations in Chapter 4.

³It should be mentioned here that the second asymptotical condition, $\bar{N}_{\text{DA}} \gg L$, must be indeed taken into account. This is because the estimates of the channel coefficients, over each approximation window, are obtained from the \bar{N}_{DA} samples received over that window only. Their accuracy does not depend, therefore, on how many samples are received outside that approximation window (the rest of the observation window). Yet, the size of the whole observation window, N , will ultimately affect the performance of the SNR estimator through the noise variance estimate (that is indeed obtained from all the received samples).

3.2.3 Derivation of the DA CRLB

To assess the performance of the new unbiased DA ML estimator, we need to compare its variance to a theoretical lower bound. Thus, we will also derive the corresponding CRLB.

To do so, we define the following parameter vector:

$$\boldsymbol{\theta}' = [\boldsymbol{\alpha}^T, \boldsymbol{\beta}^T, \sigma^2]^T \quad (3.30)$$

where $\boldsymbol{\alpha} = \Re\{\mathbf{h}\}$ and $\boldsymbol{\beta} = \Im\{\mathbf{h}\}$ denote the real and imaginary parts of the vector $\mathbf{h} = [\mathbf{h}_1^T, \mathbf{h}_2^T, \dots, \mathbf{h}_{N_r}^T]^T$ that contains the true channel coefficients over all the receiving antenna elements and the entire observation window. The CRLB for the DA SNR estimation over the i^{th} antenna is given by:

$$\text{CRLB}_{\text{DA}}(\rho_i) = \left(\frac{\partial \rho_i}{\partial \boldsymbol{\theta}'} \right)^T \mathbf{I}_{\text{DA}}^{-1}(\boldsymbol{\theta}') \left(\frac{\partial \rho_i}{\partial \boldsymbol{\theta}'} \right) \quad (3.31)$$

where $\rho_i = \mathbf{h}_i^H \mathbf{h}_i / N(2\sigma^2)$ and $\mathbf{I}_{\text{DA}}(\boldsymbol{\theta}')$ denotes the Fisher information matrix (FIM) whose entries are defined as:

$$[\mathbf{I}_{\text{DA}}(\boldsymbol{\theta}')]_{i,l} = -\mathbb{E}_{\mathbf{y}_{\text{DA}}} \left\{ \frac{\partial^2 \ln(P(\mathbf{y}_{\text{DA}}; \boldsymbol{\theta}'))}{\partial \boldsymbol{\theta}'_i \partial \boldsymbol{\theta}'_l} \right\} \quad (3.32)$$

where

$$P(\mathbf{y}_{\text{DA}}; \boldsymbol{\theta}') = \prod_{i=1}^{N_r} \frac{1}{(2\pi\sigma^2)^N} \exp \left\{ -\frac{(\mathbf{y}_{i,\text{DA}} - \mathbf{A}\mathbf{h}_i)^H (\mathbf{y}_{i,\text{DA}} - \mathbf{A}\mathbf{h}_i)}{2\sigma^2} \right\} \quad (3.33)$$

in which \mathbf{A} is a diagonal matrix containing the N transmitted pilot symbols. The analytical expression above for the FIM is derived in the Appendix. Moreover, by noting that that $\rho_i = \mathbf{h}_i^H \mathbf{h}_i / N(2\sigma^2)$ and $\mathbf{h}_i = \boldsymbol{\alpha}_i + j\boldsymbol{\beta}_i$, it is easy to verify that:

$$\rho_i = \frac{\boldsymbol{\alpha}_i^T \boldsymbol{\alpha}_i + \boldsymbol{\beta}_i^T \boldsymbol{\beta}_i}{N(2\sigma^2)} \quad (3.34)$$

from which we have:

$$\frac{\partial \rho_i}{\partial \boldsymbol{\alpha}_i} = \frac{\boldsymbol{\alpha}_i}{N\sigma^2}, \quad \frac{\partial \rho_i}{\partial \boldsymbol{\beta}_i} = \frac{\boldsymbol{\beta}_i}{N\sigma^2}, \quad \frac{\partial \rho_i}{\partial \sigma^2} = \frac{-\mathbf{h}_i^H \mathbf{h}_i}{2N\sigma^4} \quad (3.35)$$

and $\partial \rho_i / \partial \boldsymbol{\alpha}_l = \partial \rho_i / \partial \boldsymbol{\beta}_l = \mathbf{0}_{1 \times L}$ for $i \neq l$. Using (3.35) and the results enclosed in the Appendix, a simple closed-form expression for the DA CRLB over the i^{th} antenna branch is obtained as follows:

$$\text{CRLB}_{\text{DA}}(\rho_i) = \frac{\rho_i}{N} \left(2 + \frac{\rho_i}{N_r} \right). \quad (3.36)$$

Now, it becomes clear that the right-hand side of (3.29) is nothing but the CRLB of the underlying estimation problem. Moreover, even though this bound was primarily derived for the DA scenario, it also holds in the NDA case, for moderate to high SNR values. This is hardly surprising since in this SNR region the NDA algorithm (developed in the next section) is able to perfectly estimate the unknown transmitted symbols reaching thereby the DA performance.

3.3 Formulation of the new NDA ML SNR estimator

3.3.1 New NDA ML SNR Estimator

In this section, we derive the new NDA ML SNR estimator where a partial *a priori* knowledge of the transmitted symbols is assumed at the receiver. To begin with, we mention that the problem formulation adopted in the DA case is problematic in the NDA scenario. In fact, as will be seen shortly, the EM algorithm averages the likelihood function, at each iteration, over all the possible values of the *complete* data (which are the unknown transmitted symbols).

Consequently, by adopting the same previous formulation, the EM algorithm would average over all the possible realizations of the matrix \mathbf{B} that contains these *complete* data. This results in a combinatorial problem with prohibitive (i.e., exponentially increasing) complexity. In the DA scenario, this was feasible since the matrix \mathbf{B} (or the transmitted sequence) is *a priori* known to the receiver and no averaging was required. Thus, we reformulate our system differently so that the EM algorithm averages over the elementary symbols transmitted at separate time instants. In this way, the complexity of the algorithm becomes only linear with the modulation order.

To that end, we define⁴ the vector $\mathbf{t}(n) = [1, t_n, t_n^2, \dots, t_n^{L-1}]^T$ which is the n^{th} row (transposed to a column vector) of the Vandermond matrix \mathbf{T} defined as:

$$\mathbf{T} = \begin{pmatrix} 1 & t_1 & \cdots & t_1^{L-1} \\ 1 & t_2 & \cdots & t_2^{L-1} \\ \vdots & \vdots & \ddots & \vdots \\ 1 & t_N & \cdots & t_{N_{\text{NDA}}}^{L-1} \end{pmatrix} \quad (3.37)$$

and rewrite the channel model as follows:

$$\begin{aligned} h_{i,k}(t_n) &= \sum_{l=0}^{L-1} c_{i,k}^{(l)} t_n^l \\ &= \mathbf{c}_{i,k}^T \mathbf{t}(n). \end{aligned} \quad (3.38)$$

⁴We mention that, for ease of notation, we will from now on use $\mathbf{t}(n)$ instead of $\mathbf{t}(nT_s)$. For the same reasons, we will keep dropping T_s in all similar quantities.

At each time instant n (whithin the k^{th} approximation window of size⁵ $\bar{N} = \bar{N}_{\text{NDA}}$), we take all the received samples at the output of the antennae array, $\{y_{i,k}(n)\}_{i=1}^{N_r}$, (usually called *snapshot* in array signal processing terminology) and we stack them into a single vector, $\mathbf{y}_k(n) = [y_{1,k}(n), y_{2,k}(n), \dots, y_{N_r,k}(n)]^T$, which can be expressed as:

$$\mathbf{y}_k(n) = a_k(n)\mathbf{C}_k\mathbf{t}(n) + \mathbf{w}_k(n) \quad (3.39)$$

in which $a_k(n)$ is the corresponding unknown transmitted symbol, $\mathbf{C}_k = [\mathbf{c}_{1,k}, \mathbf{c}_{2,k}, \dots, \mathbf{c}_{N_r,k}]^T$ and $\mathbf{w}_k(n) = [w_{1,k}(n), w_{2,k}(n), \dots, w_{N_r,k}(n)]^T$. The vectors $\mathbf{c}_{i,k}$ were defined previously in (3.8). From (3.39), the pdf of the received vector, $\mathbf{y}_k(n)$, conditioned on the transmitted symbol $a_k(n)$, can be expressed as the product of its element-wise pdfs as follows:

$$p(\mathbf{y}_k(n); \boldsymbol{\theta}_k | a_k(n) = a_m) = \prod_{i=1}^{N_r} \frac{1}{2\pi\sigma^2} \exp \left\{ -\frac{1}{2\sigma^2} |y_{i,k}(n) - a_m \mathbf{c}_{i,k}^T \mathbf{t}(n)|^2 \right\} \quad (3.40)$$

in which a_m is the *hypothetically* transmitted symbol that is randomly drawn from the M -ary constellation alphabet $\mathcal{C} = \{a_1, a_2, \dots, a_M\}$. Now, averaging (3.40) over this alphabet and assuming the transmitted symbols to be equally likely, i.e., $P[a_m] = 1/M$ for $m = 1, 2, \dots, M$, the pdf of the received vector is obtained as:

$$p(\mathbf{y}_k(n); \boldsymbol{\theta}_k) = \frac{1}{M} \sum_{m=1}^M \prod_{i=1}^{N_r} \frac{1}{2\pi\sigma^2} \exp \left\{ -\frac{1}{2\sigma^2} |y_{i,k}(n) - a_m \mathbf{c}_{i,k}^T \mathbf{t}(n)|^2 \right\}. \quad (3.41)$$

By inspecting (3.41), it becomes clear that a joint maximization of the likelihood function, with respect to σ^2 and $\{\mathbf{c}_{i,k}\}_{i=1}^{N_r}$, is analytically intractable. Yet, this multidimensional optimization problem can be efficiently tackled using the EM concept. Indeed, given the

⁵Note also that we may use a different size for the local approximation windows in the NDA scenario, i.e., \bar{N}_{DA} may be different from \bar{N}_{NDA} .

so-called “*incomplete* data set” in EM terminology (the available observation samples in our case), the log-likelihood function conditioned on the *complete* data (transmitted symbol), $L(\boldsymbol{\theta}_k | a_k(n) = a_m) = \ln(p(\mathbf{y}_k(n); \boldsymbol{\theta}_k | a_k(n) = a_m))$ is given by:

$$\begin{aligned} L(\boldsymbol{\theta}_k | a_k(n) = a_m) &= -N_r \ln(2\pi\sigma^2) - \frac{1}{2\sigma^2} \sum_{i=1}^{N_r} |y_{i,k}(n) - a_m \mathbf{c}_{i,k}^T \mathbf{t}(n)|^2 \\ &= -N_r \ln(2\pi\sigma^2) - \frac{1}{2\sigma^2} \sum_{i=1}^{N_r} \left(|y_{i,k}(n)|^2 + |a_m|^2 |\mathbf{c}_{i,k}^T \mathbf{t}(n)|^2 \right. \\ &\quad \left. - 2\Re \{ y_{i,k}^*(n) a_m \mathbf{c}_{i,k}^T \mathbf{t}(n) \} \right). \end{aligned} \quad (3.42)$$

The new EM-based algorithm runs in two main steps. During the “expectation step” (E-step), the expected value of the above likelihood function with respect to all the possible transmitted symbols $\{a_m\}_{m=1}^M$ is computed. Then, during the “maximization step” (M-step), the output of the E-step is maximized with respect to all the unknown parameters. The E-step is established as follows: starting from an initial guess⁶, $\hat{\boldsymbol{\theta}}_k^{(0)}$, about the unknown parameter vector, the objective function is updated iteratively according to:

$$Q(\boldsymbol{\theta}_k | \hat{\boldsymbol{\theta}}_k^{(q-1)}) = \sum_{n=1}^{\bar{N}_{\text{NDA}}} E_{a_m} \left\{ L(\boldsymbol{\theta}_k | a(n) = a_m) \Big| \hat{\boldsymbol{\theta}}_k^{(q-1)}, \mathbf{y}_k(n) \right\} \quad (3.43)$$

where $E_{a_m}\{\cdot\}$ is the expectation over all possible transmitted symbols a_m , and $\hat{\boldsymbol{\theta}}_k^{(q-1)}$ is the estimated parameter vector at the $(q-1)^{\text{th}}$ iteration. After some algebraic manipulations, it can be shown that:

$$Q(\boldsymbol{\theta}_k | \hat{\boldsymbol{\theta}}_k^{(q-1)}) = -\bar{N}_{\text{NDA}} N_r \ln(2\pi\sigma^2) - \frac{1}{2\sigma^2} \sum_{i=1}^{N_r} \left(M_{2,k}^{(i)} + \sum_{n=1}^{\bar{N}_{\text{NDA}}} \alpha_{n,k}^{(q-1)} |\mathbf{c}_{i,k}^T \mathbf{t}(n)|^2 - 2\beta_{i,n,k}^{(q-1)}(\mathbf{c}_{i,k}) \right) \quad (3.44)$$

⁶The initialization issues are very critical to the convergence of the new iterative NDA algorithm. They will be discussed in more details at the end of this subsection.

where $M_{2,k}^{(i)} = E\{|y_{i,k}(n)|^2\}$ is the second-order moment of the received samples over the i^{th} receiving antenna element and:

$$\alpha_{n,k}^{(q-1)} = E_{a_m} \left\{ |a_m|^2 \middle| \hat{\boldsymbol{\theta}}_k^{(q-1)}, \mathbf{y}_k(n) \right\} \quad (3.45)$$

$$= \sum_{m=1}^M P_{m,n,k}^{(q-1)} |a_m|^2, \quad (3.46)$$

$$\begin{aligned} \beta_{i,n,k}^{(q-1)}(\mathbf{c}_{i,k}) &= E_{a_m} \left\{ \Re \{ y_{i,k}^*(n) a_m \mathbf{t}^T(n) \mathbf{c}_{i,k} \} \middle| \hat{\boldsymbol{\theta}}_k^{(q-1)}, \mathbf{y}_k(n) \right\} \\ &= \sum_{m=1}^M P_{m,n,k}^{(q-1)} \Re \{ y_{i,k}^*(n) a_m \mathbf{t}^T(n) \mathbf{c}_{i,k} \}. \end{aligned} \quad (3.47)$$

In (3.45) and (3.47), $P_{m,n,k}^{(q-1)} = P(a_m | \mathbf{y}_k(n); \hat{\boldsymbol{\theta}}_k^{(q-1)})$ is the *a posteriori* probability of a_m at iteration $(q-1)$ that can be computed using the Bayes formula as follows:

$$P_{m,n,k}^{(q-1)} = \frac{P[a_m] P(\mathbf{y}_k(n) | a_m; \hat{\boldsymbol{\theta}}_k^{(q-1)})}{P(\mathbf{y}_k(n); \hat{\boldsymbol{\theta}}_k^{(q-1)})}. \quad (3.48)$$

Since the transmitted symbols are equally likely, we have $P[a_m] = 1/M$, and thus:

$$P(\mathbf{y}_k(n); \hat{\boldsymbol{\theta}}_k^{(q-1)}) = \frac{1}{M} \sum_{m=1}^M P(\mathbf{y}_k(n) | a_m; \hat{\boldsymbol{\theta}}_k^{(q-1)}). \quad (3.49)$$

In the special case of constant-envelope constellations (such as MPSK), we have $|a_m|^2 = 1$ for all $a_m \in \mathcal{C}$ and, therefore, $\alpha_k^{(q-1)}(n)$ reduces simply to one for all n and does not need to be computed. Now, the M-step can be fulfilled by determining the parameters that maximize the output of the E-step, obtained in (3.44):

$$\hat{\boldsymbol{\theta}}_k^{(q)} = \arg \max_{\boldsymbol{\theta}_k} Q(\boldsymbol{\theta}_k | \hat{\boldsymbol{\theta}}_k^{(q-1)}). \quad (3.50)$$

At this stage, in order to avoid the cumbersome differentiation of the underlying objective function with respect to the complex vectors, $\{\mathbf{c}_{i,k}\}_{i=1}^{N_r}$, we split them into $\mathbf{c}_{i,k} = \Re\{\mathbf{c}_{i,k}\} +$

$j\Im\{\mathbf{c}_{i,k}\}$. We then instead maximize $Q\left(\boldsymbol{\theta}_k|\widehat{\boldsymbol{\theta}}_k^{(q-1)}\right)$ with respect to $\Re\{\mathbf{c}_{i,k}\}$ and $\Im\{\mathbf{c}_{i,k}\}$ yielding thereby, at the convergence of the iterative algorithm, their respective ML estimates $\Re\{\widehat{\mathbf{c}}_{i,k}\}$ and $\Im\{\widehat{\mathbf{c}}_{i,k}\}$. Then, by the invariance principle of the maximum likelihood estimator, we easily obtain the NDA ML estimate of $\mathbf{c}_{i,k}$ as $\widehat{\mathbf{c}}_{i,k} = \Re\{\widehat{\mathbf{c}}_{i,k}\} + j\Im\{\widehat{\mathbf{c}}_{i,k}\}$. Therefore, starting from (3.44) and after some algebraic manipulations, it can be shown that :

$$Q\left(\boldsymbol{\theta}_k|\widehat{\boldsymbol{\theta}}_k^{(q-1)}\right) = -\bar{N}_{\text{NDA}}N_r \ln(2\pi\sigma^2) - \frac{1}{2\sigma^2} \sum_{i=1}^{N_r} \left[M_{2,k}^{(i)} + \sum_{n=1}^{\bar{N}_{\text{NDA}}} \left(\mathbf{t}^T(n) \mathbf{C}_{i,k} \mathbf{t}(n) - 2 \sum_{m=1}^M P_{m,n,k}^{(q-1)} \tilde{\mathbf{c}}_{i,k}^{(m)T} \mathbf{t}(n) \right) \right]. \quad (3.51)$$

where $\mathbf{C}_{i,k}$ and $\tilde{\mathbf{c}}_{i,k}^{(m)}$ are, respectively, a matrix and a column vector that are explicitly constructed from the real and imaginary parts of $\mathbf{c}_{i,k}$ as follows:

$$\mathbf{C}_{i,k} = \Re\{\mathbf{c}_{i,k}\}\Re\{\mathbf{c}_{i,k}\}^T + \Im\{\mathbf{c}_{i,k}\}\Im\{\mathbf{c}_{i,k}\}^T + j\left(\Re\{\mathbf{c}_{i,k}\}\Im\{\mathbf{c}_{i,k}\}^T - \Im\{\mathbf{c}_{i,k}\}\Re\{\mathbf{c}_{i,k}\}^T\right), \quad (3.52)$$

$$\tilde{\mathbf{c}}_{i,k}^{(m)} = \Re\{y_{i,k}^*(n)a_m\}\Re\{\mathbf{c}_{i,k}\} + \Im\{y_{i,k}^*(n)a_m\}\Im\{\mathbf{c}_{i,k}\}. \quad (3.53)$$

After differentiating (3.51) with respect to $\Re\{\mathbf{c}_{i,k}\}$ and $\Im\{\mathbf{c}_{i,k}\}$, and setting the resulting equations to zero, we obtain the NDA estimates of the real and imaginary parts of $\mathbf{c}_{i,k}$, at the q^{th} iteration, as follows:

$$\Re\{\widehat{\mathbf{c}}_{i,k}^{(q)}\} = \left(\sum_{n=1}^{\bar{N}_{\text{NDA}}} \mathbf{t}(n)\mathbf{t}^T(n) \right)^{-1} \left(\sum_{n=1}^{\bar{N}_{\text{NDA}}} \sum_{m=1}^M P_{m,n,k}^{(q-1)} \Re\{y_{i,k}^*(n)a_m\} \mathbf{t}(n) \right), \quad (3.54)$$

and

$$\Im\{\widehat{\mathbf{c}}_{i,k}^{(q)}\} = \left(\sum_{n=1}^{\bar{N}_{\text{NDA}}} \mathbf{t}(n)\mathbf{t}^T(n) \right)^{-1} \left(\sum_{n=1}^{\bar{N}_{\text{NDA}}} \sum_{m=1}^M P_{m,n,k}^{(q-1)} \Im\{y_{i,k}^*(n)a_m\} \mathbf{t}(n) \right). \quad (3.55)$$

Then, using the identity $\widehat{\mathbf{c}}_{i,k}^{(q)} = \Re\{\widehat{\mathbf{c}}_{i,k}^{(q)}\} + j\Im\{\widehat{\mathbf{c}}_{i,k}^{(q)}\}$ and after some simplifications we derive the expression of $\widehat{\mathbf{c}}_{i,k}^{(q)}$ as follows:

$$\widehat{\mathbf{c}}_{i,k}^{(q)} = \left(\sum_{n=1}^{\bar{N}_{\text{NDA}}} \mathbf{t}(n)\mathbf{t}^T(n) \right)^{-1} \left(\sum_{n=1}^{\bar{N}_{\text{NDA}}} \lambda_{i,n,k}^{(q-1)} \mathbf{t}(n) \right) \quad (3.56)$$

where:

$$\lambda_{i,n,k}^{(q-1)} = \left(\underbrace{\sum_{m=1}^M P_{m,n,k}^{(q-1)} a_m}_{\widehat{a}_k^{(q-1)}(n)} \right)^* y_{i,k}(n) \quad (3.57)$$

$$= \widehat{a}_k^{(q-1)}(n)^* y_{i,k}(n) \quad (3.58)$$

in which $\widehat{a}_k^{(q-1)}(n)$ is the previous *soft* estimate for the unknown transmitted symbol, $a_k(n)$, involved in (3.39). In fact, at each time instant n , all the constellation points are scanned and their *a posteriori* probabilities, $P_{m,n,k}$, are updated from one iteration to another. At convergence of the algorithm, the probabilities of the wrong symbols are nulled and the weighted sum involved in (3.57) returns the actual transmitted symbol. More specifically, assume that the symbol a_{m_0} is transmitted at time instant n during the approximation window k , i.e., $a_k(n) = a_{m_0}$. At the convergence (we drop therefore the iteration index q) and especially for moderate-to-high SNR values, the *a posteriori* probabilities satisfy $P_{m,n,k} \approx 0$ for $m \neq m_0$ and $P_{m_0,n,k} \approx 1$. Hence, from (3.57), it follows that:

$$\widehat{a}_k(n) = \sum_{m=1}^M P_{m,n,k} a_m \approx a_{m_0} = a_k(n), \quad (3.59)$$

meaning that the algorithm succeeds in correctly “decoding” all the transmitted symbols. Lastly, by differentiating (3.51) with respect to σ^2 , setting the resulting equation to zero, and replacing in it $\mathbf{c}_{i,k}$ by $\widehat{\mathbf{c}}_{i,k}^{(q-1)}$, we obtain a new estimate for the noise power at the q^{th}

iteration as follows:

$$2\widehat{\sigma}_k^{(q)} = \frac{\sum_{i=1}^{N_r} \left(M_{2,k}^{(i)} + \eta_{i,k}^{(q-1)} \right)}{\bar{N}_{\text{NDA}} N_r}, \quad (3.60)$$

where:

$$\begin{aligned} \eta_{i,k}^{(q-1)} &= \sum_{n=1}^{\bar{N}_{\text{NDA}}} \left[\mathbf{t}^T(n) \left(\widehat{\mathbf{c}}_{i,k}^{(q-1)} \right)^* \left(\widehat{\mathbf{c}}_{i,k}^{(q-1)} \right)^T \mathbf{t}(n) + \alpha_{n,k}^{(q-1)} - 2\beta_{i,n,k}^{(q-1)} \left(\widehat{\mathbf{c}}_{i,k}^{(q-1)} \right) \right] \\ &= \sum_{n=1}^{\bar{N}_{\text{NDA}}} \left[\left| \mathbf{t}^T(n) \widehat{\mathbf{c}}_{i,k}^{(q-1)} \right|^2 + \alpha_{n,k}^{(q-1)} - 2\beta_{i,n,k}^{(q-1)} \left(\widehat{\mathbf{c}}_{i,k}^{(q-1)} \right) \right]. \end{aligned} \quad (3.61)$$

After a few iterations (i.e., in the range of 10), the EM algorithm converges — over each approximation window k — to the exact NDA ML estimates $\widehat{\mathbf{c}}_{i,\text{NDA}}^{(k)}$ and $\widehat{\sigma}_{k,\text{NDA}}^2$. The latter is then averaged over all the local approximation windows to obtain a more refined estimate as follows:

$$\widehat{\sigma}_{\text{NDA}}^2 = \frac{\bar{N}_{\text{NDA}}}{N} \sum_{k=1}^{N/\bar{N}_{\text{NDA}}} \widehat{\sigma}_{k,\text{NDA}}^2. \quad (3.62)$$

Finally, given (3.56) and (3.62), and taking into account all the approximation windows of size \bar{N}_{NDA} within the same observation window of size N , the NDA ML SNR estimator is obtained as:

$$\widehat{\rho}_{i,\text{NDA}} = \frac{\sum_{k=1}^{N/\bar{N}_{\text{NDA}}} \sum_{n=1}^{\bar{N}_{\text{NDA}}} \left| \mathbf{t}^T(n) \widehat{\mathbf{c}}_{i,\text{NDA}}^{(k)} \right|^2}{N \left(2\widehat{\sigma}_{\text{NDA}}^2 \right)}. \quad (3.63)$$

Now, recall that the EM algorithm is iterative in nature and, therefore, its performance is closely tied to the initial guess $\widehat{\boldsymbol{\theta}}_k^{(0)}$ within each approximation window. We will see in the next Chapter that when it is not appropriately initialized, its performance is indeed severely affected, especially at high SNR levels. This is actually a serious problem inherent to any iterative algorithm whose objective function is not convex. That is, it may settle on

a local maximum if it happens that the algorithm is accidentally initialized around it. Yet, an appropriate initial guess about the polynomial coefficients, $\widehat{\mathbf{c}}_{i,k}^{(0)}$, and the noise variance, $\widehat{\sigma}^2^{(0)}$, can be locally acquired using very few pilot symbols by applying the DA ML estimator developed in the previous section.

Therefore, we will henceforth use two different designations for the new EM-based estimator according to the initialization procedure. We shall refer to it as “*completely NDA*” if it is initialized *arbitrarily* and as “*hybrid NDA*” when it is *appropriately* initialized using the DA estimator. It should also be noted that, depending on the simulation scenario, we use two different designations for the DA estimator. On one hand, we refer to it as “*pilot-only DA*” when applied using the pilot symbols only (which are N/N_p out of the N transmitted symbols with $N_p > 1$). On the other hand, we refer to it as “*completely DA*” when applied in a rather hypothetical scenario in which all the N transmitted symbols are assumed to be perfectly known (i.e., $N_p = 1$). The latter is of course with limited practical use⁷ and considered here only as an ideal benchmark, along with the DA CRLB, against which the performance of all the other practical estimators are compared.

In order to initialize the EM algorithm with the DA estimates, we proceed as follows. Using the pilot symbols only, we begin by estimating the channel coefficients using the DA estimator over local approximation windows of size \bar{N}_{DA} . Over each antenna element, these pilot-based DA estimates are then stacked together to form a single vector that contains

⁷Actually, in some radio interface technologies such as CDMA, a pilot channel is considered with a completely known data sequence. In OFDM, some carriers might bear completely known data sequences as well.

all the pilot-based estimates of the channel coefficients, $\hat{\mathbf{h}}_{i,\text{DA}}$ (over the entire observation window). The latter is then divided into several adjacent and disjoint blocks, $\hat{\mathbf{h}}_{i,\text{DA}}^{(k)}$, each of size \bar{N}_{NDA} (possibly different from \bar{N}_{DA}). Then, according to (3.38), the initial guess about the polynomial coefficients, within the k^{th} local NDA approximation window, is obtained from the k^{th} block using $\hat{\mathbf{c}}_{i,k}^{(0)} = (\mathbf{T}^T \mathbf{T})^{-1} \mathbf{T} \hat{\mathbf{h}}_{i,\text{DA}}^{(k)}$. The initial guess about the noise variance is simply $\hat{\sigma}^2{}^{(0)} = \hat{\sigma}_{\text{DA}}^2$ obtained in (3.19).

If carefully handled⁸, the *hybrid* NDA EM-based estimator always converges to the global maximum of the likelihood function for moderate-to-high SNR values and, as mentioned previously, it is able to correctly detect all the unknown symbols. Therefore, in this SNR region, it is equivalent in performance to the biased “*completely DA*” estimator. Therefore, the same bias-correction procedure highlighted earlier in (3.28) can be exploited here as well by using $\epsilon = L/\bar{N}_{\text{NDA}}$.

3.3.2 The previously presented work (*WL*) and its SIMO extension

The only work that considered time-varying ML SNR estimation is the one of [18]. Therefore, we present the results obtained therein in its original SISO configuration as well as its SIMO extension so that we can compare it to our estimator performance. Consider the i^{th} antenna

⁸This requires careful choices of the approximation window size, of both the hybrid NDA estimator and the DA estimator used to initialize it with respect to the normalized Doppler frequency $F_D T_s$. These optimal Doppler-dependent choices were found and reported in table 4.1 at the end of the next Chapter.

element separately, as presented in [18], the estimated SNR is given by:

$$\hat{\rho}_i = \frac{\mathbf{y}_i^H \mathbf{P} \mathbf{y}_i}{\mathbf{y}_i^H \mathbf{P}^\perp \mathbf{y}_i}, \quad (3.64)$$

where $\mathbf{P} = \hat{\mathbf{A}} \mathbf{T} (\mathbf{T}^T \mathbf{T})^{-1} \mathbf{T}^T \hat{\mathbf{A}}^H$ and $\mathbf{P}^\perp = \mathbf{I} - \mathbf{P}$ are projection matrices onto the signal-plus-noise and noise-only subspaces respectively. $\hat{\mathbf{A}}^H$ is a diagonal matrix whose entries are given by:

$$[\hat{\mathbf{A}}]_{nn}^H = \mathbb{E}\{a(n)|y_i(n); \boldsymbol{\theta}\}. \quad (3.65)$$

The elements of $\hat{\mathbf{A}}^H$ were derived in closed form in [18] for BPSK constellation only:

$$[\hat{\mathbf{A}}]_{nn}^H = \tanh\left(\frac{2\Re\{y_i(n)\hat{h}_i^*(n)\}}{\hat{\sigma}^2}\right), \quad (3.66)$$

where $\tanh(\cdot)$ refers to the hyperbolic tangent function, and $\hat{h}_i(n)$ is the estimated complex channel gain over the considered i^{th} antenna element given by $\hat{h}_i(n) = \mathbf{t}_n \hat{\mathbf{c}}_i$ where \mathbf{t}_n is the n^{th} row of the matrix \mathbf{T} . We also derive in this thesis the closed-form expression for the entries of this matrix for QPSK constellations as well. In fact, assuming $a(n) \in \{\pm\sqrt{(1/2)} \pm j\sqrt{(1/2)}\}$ (i.e., QPSK transmissions), and after extensive mathematical calculations enclosed in Appendix B, we show that it follows:

$$[\hat{\mathbf{A}}]_{nn}^H = \frac{1}{\sqrt{2}} \left[\tanh\left\{\frac{\sqrt{2}}{\hat{\sigma}^2} \Re\{y_i(n)\hat{h}_i^*(n)\}\right\} - j \tanh\left\{\frac{\sqrt{2}}{\hat{\sigma}^2} \Im\{y_i(n)\hat{h}_i^*(n)\}\right\} \right]. \quad (3.67)$$

As will be seen in the next chapter, this estimator will be outperformed by our newly developed SIMO ML SNR estimator, which *fully* exploits the spatial diversity, even when compared to its enhanced SIMO version, where we take advantage of the antenna gain to obtain a more refined noise variance estimate, by averaging the individual estimates over all the receiving antenna branches.

Chapter 4

Simulation Results

In this chapter, we assess the performance of our new DA and NDA ML *instantaneous* SNR estimators. All the presented results are obtained by running extensive Monte-Carlo simulations over 5000 realizations. The estimators' performance is evaluated in terms of the normalized (by the average SNR) mean square error (NMSE), which is defined as:

$$\text{NMSE}(\hat{\rho}_i) = \frac{E\{(\rho_i - \hat{\rho}_i)^2\}}{\gamma^2} \quad (4.1)$$

where $\gamma = E\{|a(n)|^2\}/(2\sigma^2)$ is the average SNR per symbol. But since the constellation energy is assumed to be normalized to one, i.e., $E\{|a(n)|^2\} = 1$, γ is simply given by $\gamma = 1/(2\sigma^2)$. For the sake of complying with a practical and timely scenario, all the simulations are conducted in the specific context of the LTE (long-term evolution) uplink for its stringent pilot design specifications. Indeed, according to the LTE uplink signalling standard, two OFDM pilot symbols are inserted at the 4th and 11th positions¹ in the time-frequency grid of each subframe (consisting of 14 OFDM symbols). We consider an observation window

¹In this way a pilot symbol is transmitted every seven OFDM symbols corresponding to $N_p = 7$.

that covers 8 consecutive subframes, i.e., $N = 112$ received samples over each subcarrier. The “*instantaneous*” SNR estimation results are presented for the first subcarrier only, but they actually hold the same irrespectively of the subcarrier index [24].

4.1 Overflow problem correction

Our estimation process will be conducted for different ranges of $f_D T_s$. This induces a problem of overflow, especially for high values of $f_D T_s$, in which when averaging all the elementary pdfs over the constellation alphabet \mathcal{C} , as in (3.41), we will be adding different values of the quantities under the exp operator, that exceed independently Matlab precision limit. To deal with this problem, one can insert a correction term, but in our case this can not do the trick, since each term must be corrected separately. To do so, we resort to the following procedure. Recall that for each possible symbol a_m from the constellation alphabet, the pdf across all the N_r receiving antenna elements can be rewritten as follows:

$$p(\mathbf{y}_k(n); \boldsymbol{\theta}_k | a_k(n) = a_m) = \frac{1}{(2\pi\sigma^2)^{N_r}} \exp \left\{ \sum_{i=1}^{N_r} -\frac{1}{2\sigma^2} |y_{i,k}(n) - a_m \mathbf{c}_{i,k}^T \mathbf{t}(n)|^2 \right\}. \quad (4.2)$$

Then, we stack all the elementary pdfs, defined above, for all possible transmitted symbols a_m , into one single vector $\mathbf{p}'(\mathbf{y}_k(n); \boldsymbol{\theta}_k) = [p(\mathbf{y}_k(n); \boldsymbol{\theta}_k | a_k(n) = a_1), p(\mathbf{y}_k(n); \boldsymbol{\theta}_k | a_k(n) = a_2), \dots, p(\mathbf{y}_k(n); \boldsymbol{\theta}_k | a_k(n) = a_M)]$. This vector can be rewritten as follows:

$$\mathbf{p}'(\mathbf{y}_k(n); \boldsymbol{\theta}_k) = \frac{1}{(2\pi\sigma^2)^{N_r}} \exp\{\mathbf{r}_{n,k}\} \quad (4.3)$$

where $\mathbf{r}_{n,k} = \left[\sum_{i=1}^{N_r} -\frac{1}{2\sigma^2} |y_{i,k}(n) - a_1 \mathbf{c}_{i,k}^T \mathbf{t}(n)|^2, \sum_{i=1}^{N_r} -\frac{1}{2\sigma^2} |y_{i,k}(n) - a_2 \mathbf{c}_{i,k}^T \mathbf{t}(n)|^2, \dots, \sum_{i=1}^{N_r} -\frac{1}{2\sigma^2} |y_{i,k}(n) - a_M \mathbf{c}_{i,k}^T \mathbf{t}(n)|^2 \right]$. Now, concentrating on $\mathbf{r}_{n,k}$, we construct a vector that contains the positions of the dominant elements of $\mathbf{r}_{n,k}$. This can be fulfilled by a simple operation:

$$\mathbf{d} = \max(\mathbf{r}_{n,k}) - \mathbf{r}_{n,k} < pl \quad (4.4)$$

where pl refers to the approximation level. In our case we take $pl = 15$. This will provide a sufficiently accurate output since it is easy to verify that $\exp\{(x + 15)\} \gg \exp(x)$. After extracting the dominant positions, our correction procedure may be limited to the corresponding values, which are now in the same range, and hence can be corrected using the same inserted term as follows:

$$\mathbf{r}'_{n,k} = \mathbf{r}_{n,k} .* \bar{\mathbf{d}} + (\mathbf{r}_{n,k} - \text{round}(\max(\mathbf{r}_{n,k}))) .* \mathbf{d} \quad (4.5)$$

where $.*$ refers to term by term multiplication, and $\bar{\mathbf{d}}$ refers to the complementary vector of \mathbf{d} . The output of (4.5) is presented as the sum of two vectors, the first one (the left hand side vector) denotes the elements of $\mathbf{r}_{n,k}$ whose values exceed the approximation level pl , and hence can be neglected. The second vector represents the elements that will be corrected using the correction term $\text{round}(\max(\mathbf{r}_{n,k}))$. The impact of this correction procedure can be noticed clearly from the following figure:

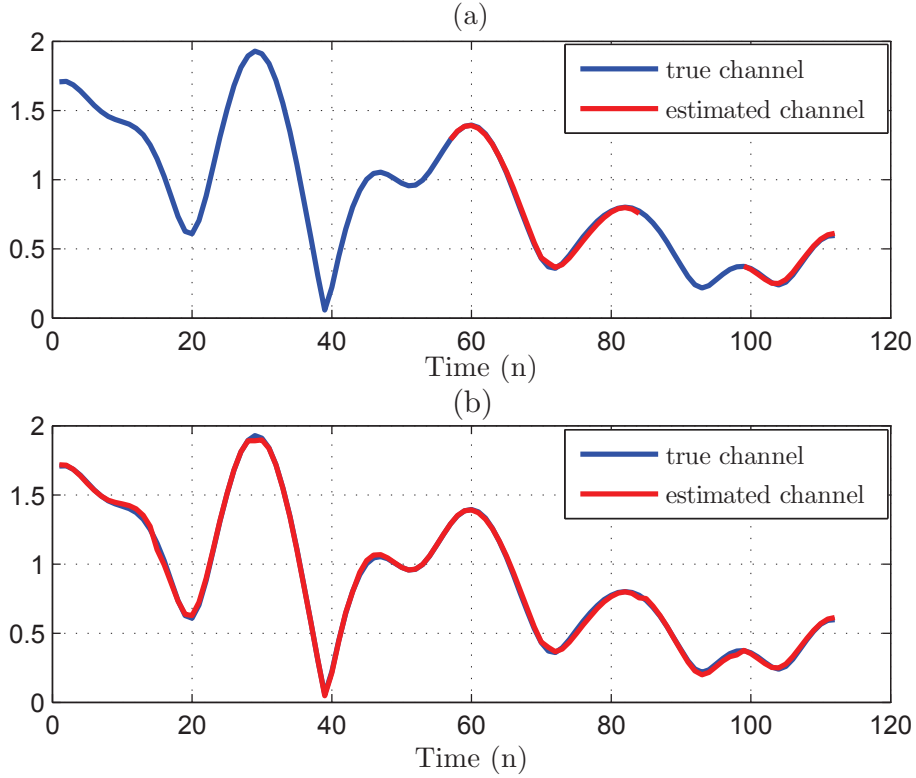


Figure 4.1: True vs. estimated channel envelope with overflow (a) and corrected-overflow (b), for $f_D T_s = 3, 5 \cdot 10^{-2}$, $N = 112$, $\bar{N}_{\text{DA}} = 28$, $\bar{N}_{\text{NDA}} = 14$ and $(L = 4)$.

4.2 Simulation results

We begin by showing the advantage of developing the NDA estimator, and applying it along with the DA estimator when it is applied on pilot symbols. In Fig. 4.2, we plot the NMSE for the “*pilot-only DA*” and the “*completely DA*” estimators as well as the “*hybrid NDA*” and “*completely NDA*” EM-based estimators (see the last section of the previous chapter for a clear definition of these different designations).

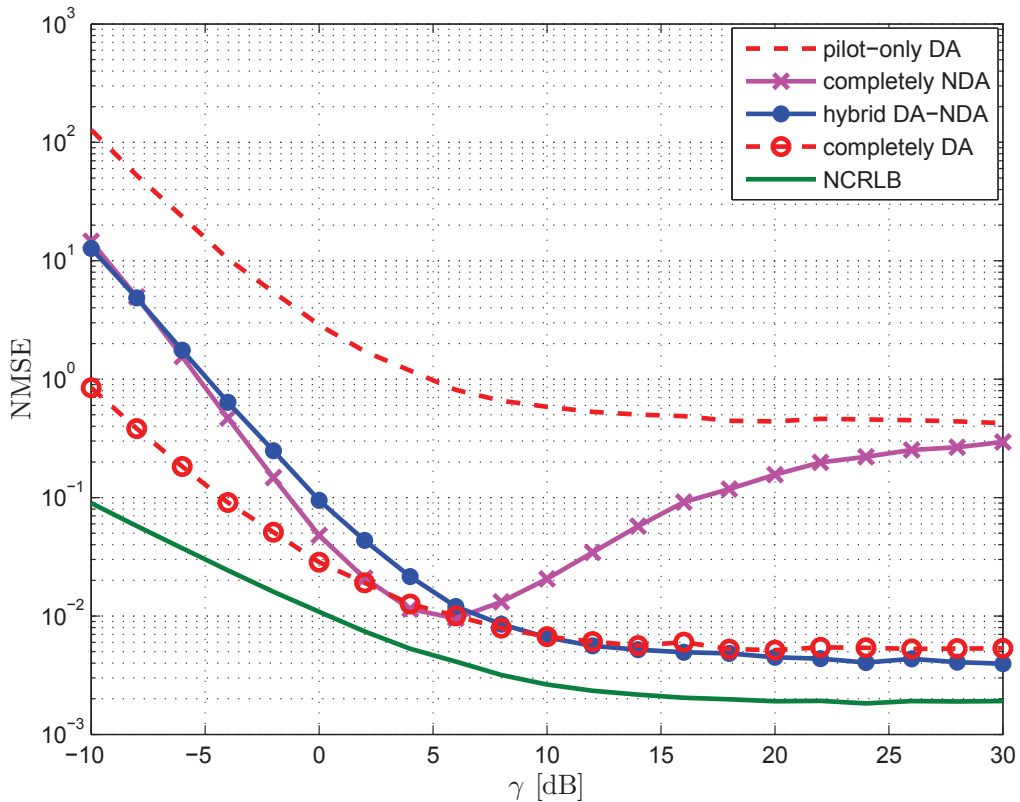


Figure 4.2: NMSE for the “*pilot-only DA*”, “*completely DA*”, “*hybrid NDA*” and “*completely NDA*” estimators vs. the average SNR γ , with $N_r = 2$, $N = 112$, $\bar{N}_{\text{DA}} = 112$, $\bar{N}_{\text{NDA}} = N/2 = 56$, $f_D T_s = 7 \cdot 10^{-3}$ and $L = 4$.

Just as mentioned earlier, it is seen that — as intuitively expected — the DA ML estimator is not able to accurately estimate the SNR by relying solely on the pilot symbols (“*pilot-only DA*”). This is due to the fast time variations of the channel. Therefore, the received samples at non-pilot positions must be used, as well, during the estimation process. Indeed, it is seen that even the “*completely NDA*” EM-based estimator is able to provide substantial performance gains at low-to-medium SNR values against the “*pilot-only DA*”

method. Yet, its performance deteriorates severely at high SNR levels due to its initialization issues. This is what makes, in turn, the “*pilot-only DA*” estimator extremely useful; even though its overall performance is not satisfactory. Indeed, its estimates are accurate enough as initial estimates for the EM-based algorithm to make it converge to the global maximum. The effect of both arbitrary and appropriate initializations on the EM-based estimates for the unknown channel coefficients is shown in Fig. 4.3. Clearly, when initialized with the “*pilot-only DA*” estimates, the iterative algorithm is able to accurately track the channel variations as seen from Fig. 4.3 (b).

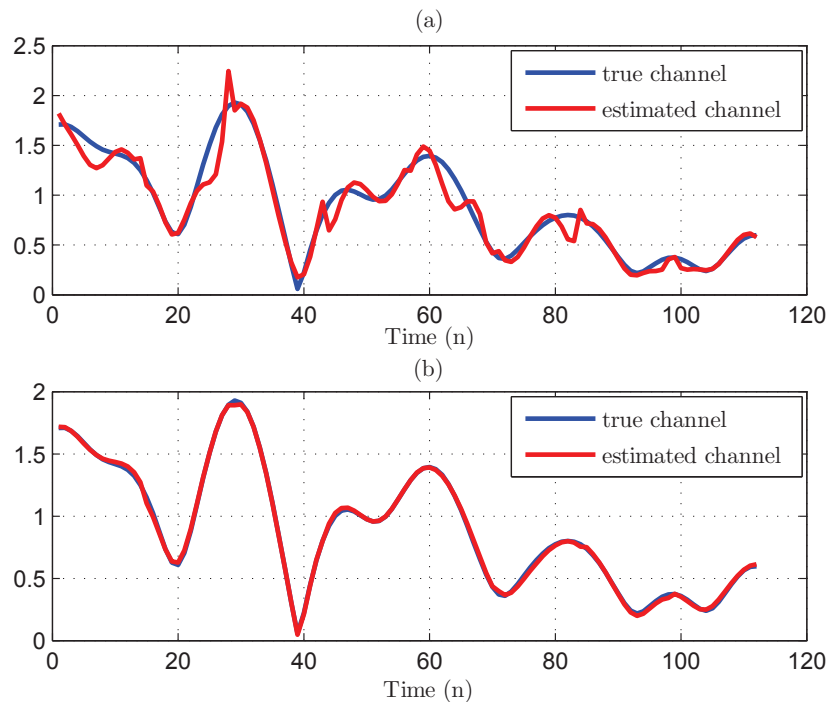


Figure 4.3: True vs. estimated channel magnitude for the EM-based algorithm when initialized (a) arbitrarily with ones, and (b) appropriately with the “*pilot-only DA*” estimates, for $f_D T_s = 3.5 \cdot 10^{-2}$, $N = 112$, $\bar{N}_{DA} = 28$, $\bar{N}_{NDA} = 14$, and $L = 4$.

Consequently², by using $\hat{\boldsymbol{\theta}}_k^{(0)} = [\hat{\mathbf{c}}_{i,k}^{(0)T} \hat{\sigma}_{\text{DA}}^2]^T$ where $\hat{\mathbf{c}}_{i,k}^{(0)} = (\mathbf{T}^T \mathbf{T})^{-1} \mathbf{T} \hat{\mathbf{h}}_{i,\text{DA}}^{(k)}$ as its starting point (or initial guess), it is observed from Fig. 4.2 that the “*hybrid NDA*” EM-based algorithm is able to accurately estimate the SNR over the entire SNR range. More interestingly, over a wide range of practical SNR (starting from SNR = 6 dB), it exhibits an estimation performance that is equivalent to the one that could be achieved if all the symbols were perfectly known (corresponding to the “*completely DA*” case). It is also seen that there is still a gap between the achieved performance and the CRLB due to the presence of an estimation bias. It will shortly be seen that this gap can also be bridged by applying the bias-correction procedure highlighted in the previous chapter.

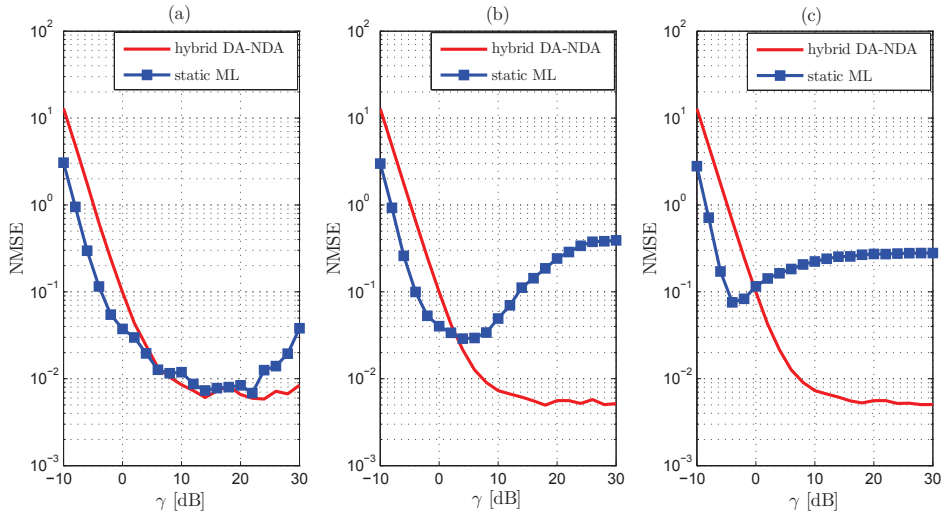


Figure 4.4: NMSE for the “*static ML*” and the “*hybrid NDA*” EM-based estimator ($L = 4$) vs. the average SNR γ , for different values of $f_D T_s$ (a) $f_D T_s = 3, 5 \cdot 10^{-4}$ (b) $f_D T_s = 3, 5 \cdot 10^{-3}$ (c) $f_D T_s = 3, 5 \cdot 10^{-2}$, with $N = 112$ and $N_r = 2$.

²See the last section of the previous chapter for more details about the pilot-assisted initialization process.

Fig. 4.4 shows that the existing NDA ML SNR estimator [14] that was primarily designed for constant or slowly time-varying SIMO channels fails completely to estimate the instantaneous SNR for fast time-varying channels. For the sake of clarity, we refer to the ML estimator of [14] as “*static ML*”. As illustrated in Fig. 4.4 (a), the “*static ML*” provides reliable estimation results especially for low SNRs ($\gamma \leq 7$ dB), and even performs better than the *hybrid* NDA DA-NDA estimator, when applied for slowly time varying channels, where $f_D T_s = 3,5 \cdot 10^{-4}$. This can be explained intuitively, since it can be noticed from (3.28) that our estimator presents a bias that can be significantly reduced by choosing a low approximation order ($L = 1$). Nevertheless, this choice results in a noticeable performance degradation in high SNR. Likewise, this performance degradation can be noticed in Fig. 4.4 (b) for a slightly wider range of SNR, in the case of faster time-varying channels ($f_D T_s = 3,5 \cdot 10^{-3}$), and even more clear in Fig. 4.4 (c), where $f_D T_s = 3,5 \cdot 10^{-2}$. This stems from the fact that this estimator is erroneously approximating the fast time-varying channels (over each antenna element) by a piecewise constant process, over each approximation window. Moreover, the “*static ML*” estimator performance degradation is due in part to the fact that it is completely blind, (without using pilot symbols for initialization). The new estimator is, however, able to track the channel variations more accurately and therefore its performance improves steadily with the average SNR.

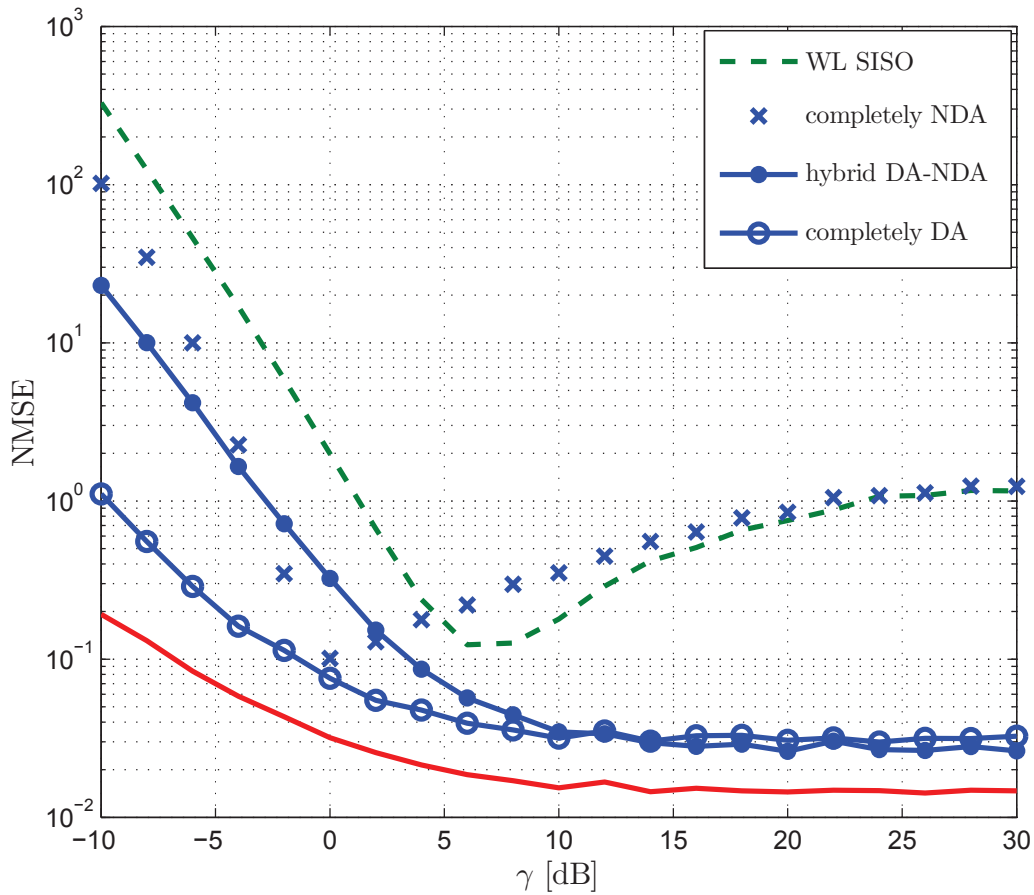


Figure 4.5: NMSE for the “*WL*”, the “*completely DA*”, the “*completely NDA*” and the *hybrid NDA* EM-based estimator ($L = 4$) and the NCRLB_{DA} vs. the average SNR γ , for SISO time-varying channels with $f_D T_s = 7 \cdot 10^{-3}$, $N = \bar{N}_{\text{DA}} = 112$, and $\bar{N}_{\text{NDA}} = 56$.

In Fig. 4.5 and 4.6, we compare our new estimator to the only reported work as far as we know on the subject of SNR estimation over time-varying channels which was introduced by A. Wiesel *et al.* in [18]. By referring to the initials of its authors’ names, we will henceforth refer to this estimator by the shorthand designation “WGL”. This estimator was originally derived for the basic single-input single-output (SISO) systems (Fig. 4.5). It can

be thus directly applied, at the output of each antenna element, in order to estimate the *instantaneous* SNR in SIMO configurations (Fig. 4.6). Yet, it can also be easily modified to take advantage of the antenna gain offered by any SIMO system experiencing *uniform* noise. In fact, over each antenna branch i , the WGL-SISO algorithm outputs two estimates; one for the signal power, \widehat{P}_i , and one for the noise power, $\widehat{N}_0^{(i)}$. The individual estimates $\{\widehat{N}_0^{(i)}\}_{i=1}^{N_r}$ can be reasonably averaged over the N_r receiving antenna elements to provide a more refined estimate, \widehat{N}_0 , for the noise power. The SIMO-enhanced SNR estimate, over each antenna element, is then computed as $\widehat{\rho}_i = \widehat{P}_i / \widehat{N}_0$. We refer to this SIMO-enhanced version as the ‘‘WGL-SIMO’’ estimator.

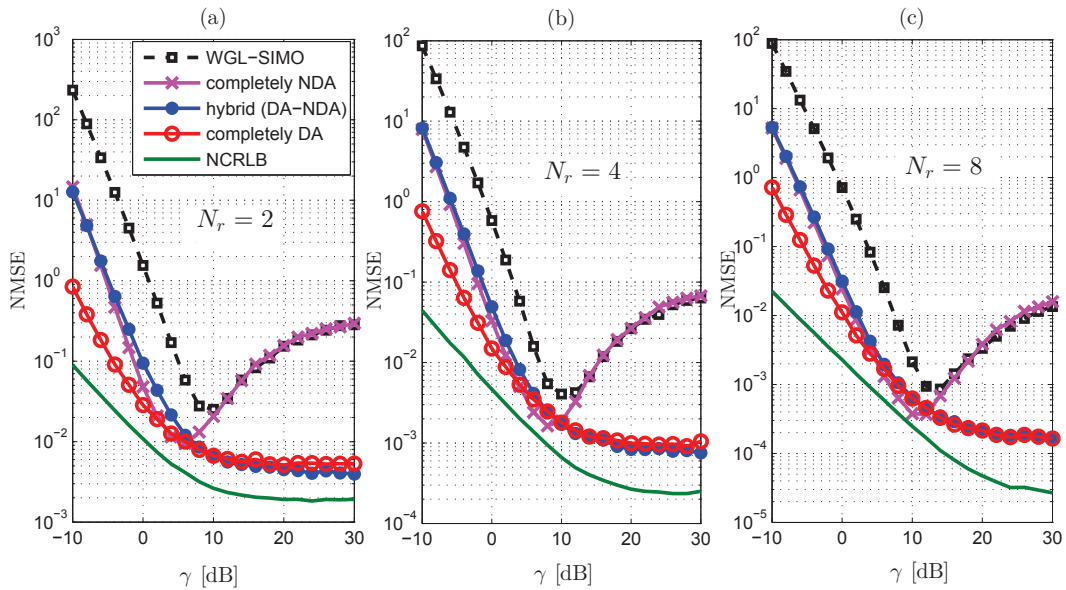


Figure 4.6: NMSE for WGL-SIMO, the ‘‘*completely DA*’’, the ‘‘*completely NDA*’’ and the *hybrid* NDA estimators vs. the average SNR γ , for $f_D T_s = 7 \cdot 10^{-3}$, $N = 112$, $\bar{N}_{\text{DA}} = 112$, and $\bar{N}_{\text{NDA}} = 56$, $L = 4$.

Fig. 4.6 depicts the performance of WGL-SIMO and the different versions of our estima-

tor for different antenna-array sizes ($N_r = 2, 4,$ and 8). First, by inspecting the behaviour of WGL-SIMO alone across the three subfigures, it is clearly seen that the performance of this new SIMO-enhanced version improves remarkably with the number of receiving antenna elements. For instance, at the typical value of the average SNR $\hat{\gamma} = 10$ dB, it is seen from Figs. 4.6 (a) and (b) that the variance of this estimator is reduced by a factor of $1/5$ when the number of antennae is doubled from $N_r = 2$ to $N_r = 4$. Almost the same improvements holds also by further doubling the array size from $N_r = 4$ to $N_r = 8$ although with a slightly smaller factor of $1/4$. These improvements are actually due to the antennae *gain*. But as WGL-SIMO is not able to exploit the antenna *diversity*, it is outperformed by both the “completely NDA” and the “*hybrid* NDA” EM-based estimators. In fact, in this thesis we make a clear difference between the two concepts of antennae *gain* and *diversity*. The former is actually inherent to all SIMO systems experiencing uniform noise across the antenna elements (whether under correlated or uncorrelated channels). In this case, averaging the N_r independent estimates of the same unknown parameter (in our case the noise variance) produces a new estimate whose variance is always shrunked by a factor of $1/N_r$ improving thereby the final estimates of the per-antenna SNRs. Antenna diversity, however, is another interesting feature of SIMO systems. Fully exploiting the antenna diversity consists in optimally combining the multiple independently-fading copies of the received signal in order to detect each of the transmitted symbols correctly. By solving the ML criterion, our EM-based estimator takes indeed advantage of the available spatial diversity during the process of accurately detecting³/estimating the unknown transmitted symbols [see (3.59)].

³Actually, the EM-based algorithm provides *soft* estimates only and does not perform a *hard* detection

The “*hybrid NDA*” EM-based algorithm outperforms, therefore, by far WGL-SIMO over the entire SNR range.

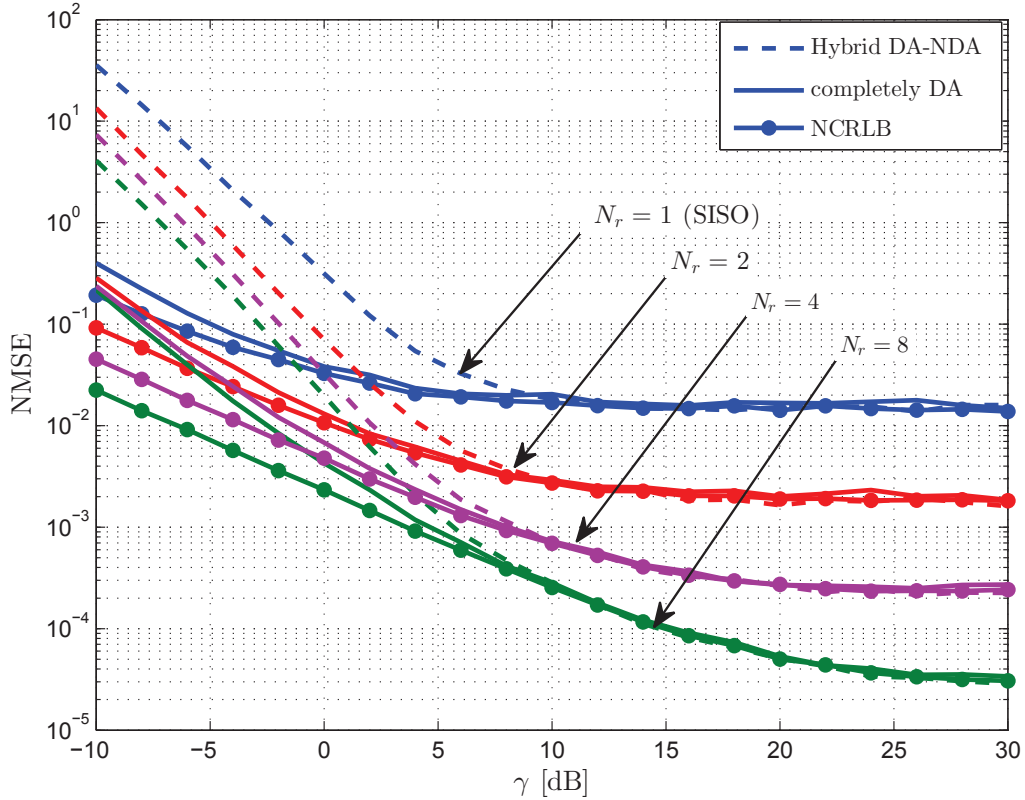


Figure 4.7: NMSE for the unbiased version of the completely DA and the hybrid estimators vs. the average SNR, for different numbers of receiving antenna elements with: $N = 112$, $\bar{N}_{\text{DA}} = 112$, $\bar{N}_{\text{NDA}} = 56$, $f_D T_s = 7 \cdot 10^{-3}$, and $L = 4$.

of the symbols. Hard detection is a separate task that may take each of these soft estimates, as input, and returns its closest symbol in the constellation alphabet. Yet, for medium-to-high SNR levels, the soft estimates returned by the “*hybrid NDA*” EM-based algorithm are very accurate and almost equal to the corresponding hard decisions. This is indeed what makes it coincide with the “*completely DA*” estimator in this SNR region.

On the other hand, it is seen from Fig. 4.6 that the gap between the CRLB and the performance of the “*completely DA*” and “*hybrid NDA*” estimators increases with the number of receiving antenna elements especially at high SNR values. This huge performance loss is actually avoidable over a wide range of practical SNRs. Indeed, in order to achieve the CRLB, the previously developed bias-correction procedure is applied and the results are plotted in Fig. 4.7. Now, over a wide SNR range, the unbiased versions of the estimators coincide with the DA CRLB that quantifies the theoretical optimal performance. Most remarkably, the “*hybrid NDA*” algorithm is able to do so while 86 % of the transmitted symbols are completely unknown (corresponding to pilot insertion rate of $1/N_p = 1/7$ in the signalling standard of the LTE uplink).

Further, this figure shows more clearly the advantage of exploiting antenna diversity, in terms of *instantaneous* SNR estimation, as compared to the SISO configuration ($N_r = 1$) plotted also in the same figure. The advantage is more prominent at medium-to-high SNR levels. For instant, at average SNR $\gamma = 30$ dB, the NMSE for $N_r = 8$ is reduced by a factor as low as 0.0004 compared to its counterpart in SISO systems.

So far, all the simulations were conducted under a normalized Doppler frequency of $f_d T_s = 7 \times 10^{-3}$ corresponding to a maximum Doppler shift $f_D = 100$ Hz with the sampling rate of LTE systems ($T_s = 70 \mu s$). Therefore, we plot in Fig. 4.8 the performance of the newly derived ML estimator (the unbiased version) for other higher normalized Doppler frequencies.

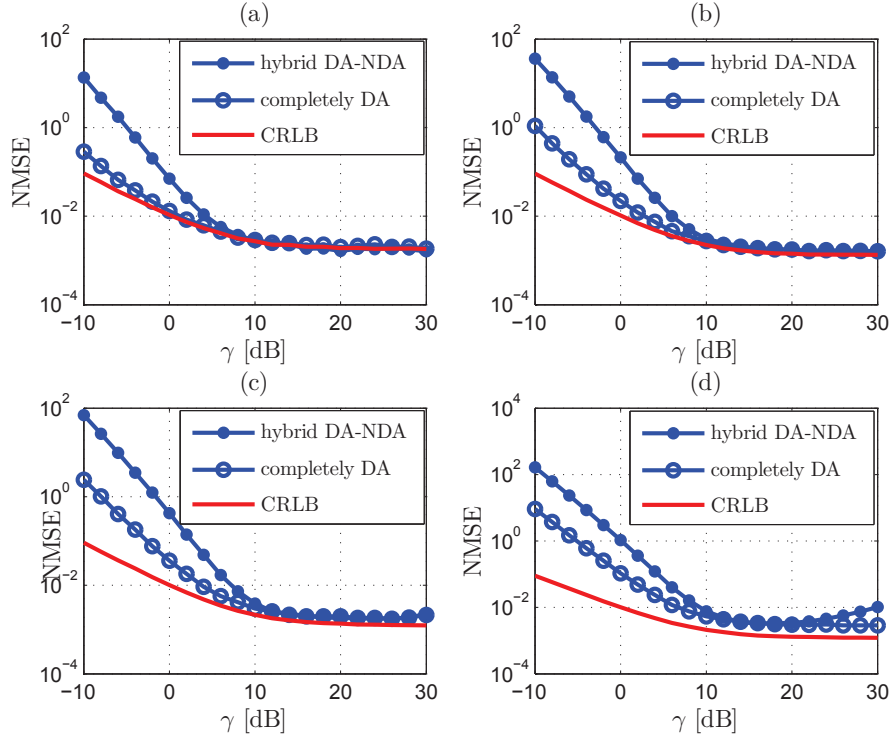


Figure 4.8: NMSE for the the “*hybrid NDA*” EM-based and the “*completely DA*” unbiased estimators vs. the average SNR with $N = 112$ and $N_r = 2$ for: (a) $f_D T_s = 7.10^{-3}$, $\bar{N}_{\text{DA}} = 112$, $\bar{N}_{\text{NDA}} = 56$, (b) $f_D T_s = 2.10^{-2}$, $\bar{N}_{\text{DA}} = 28$, $\bar{N}_{\text{NDA}} = 28$, (c) $f_D T_s = 7.10^{-3}$, $\bar{N}_{\text{DA}} = 28$, $\bar{N}_{\text{NDA}} = 14$ and (d) $f_D T_s = 7.10^{-3}$, $\bar{N}_{\text{DA}} = 14$, $\bar{N}_{\text{NDA}} = 7$.

The “*completely NDA*” estimator will not be included in the remaining simulations since is not able to estimate high SNRs. It was included in the previous figures for the sake of comparison and especially to motivate the appropriate initialization procedure using the “*pilot-only*” DA estimator. It is seen from this figure that the estimator succeeds in estimating the SNR and always reaches the CRLB over a wide range of practical SNRs even at high Doppler frequencies. In Fig. 4.8 (d), for instance, the normalized Doppler frequency is

as high as $f_D T_s = 5 \cdot 10^{-2}$ corresponding to a Doppler frequency shift of 700 Hz. We also emphasize the fact that the sizes of the local approximation windows, \bar{N}_{NDA} and \bar{N}_{DA} , for both the “*hybrid NDA*” estimator and the “*pilot-only DA*”, that is used to initialize it, should be selected as function of the Doppler range. The appropriate choices are shown in Table 4.1. In practice, the Doppler frequency can be estimated from the samples received at the pilot positions and then the approximation window sizes are selected accordingly. During the design of these Doppler-dependent configurations, our primary goal was to obtain the lowest possible polynomial orders L_{DA} and L_{NDA} which define the sizes of the two matrices that need to be inverted. Yet, it should be mentioned that these small-sizes matrices are predefined ones and, in practice, they can be computed and inverted offline. The results can then be stored, in a read-only memory, and directly used during the estimation process.

Table 4.1: local estimation configurations for different ranges of $f_D T_s$

$f_D T_s$	\bar{N}_{DA}	\bar{N}_{NDA}	L_{DA}	L_{NDA}
$7 \cdot 10^{-3} \leq$	112	56	4	4
$2 \cdot 10^{-2} \leq$	28	28	4	4
$3.5 \cdot 10^{-2} \leq$	28	14	4	4
$5 \cdot 10^{-2} \leq$	14	7	2	4

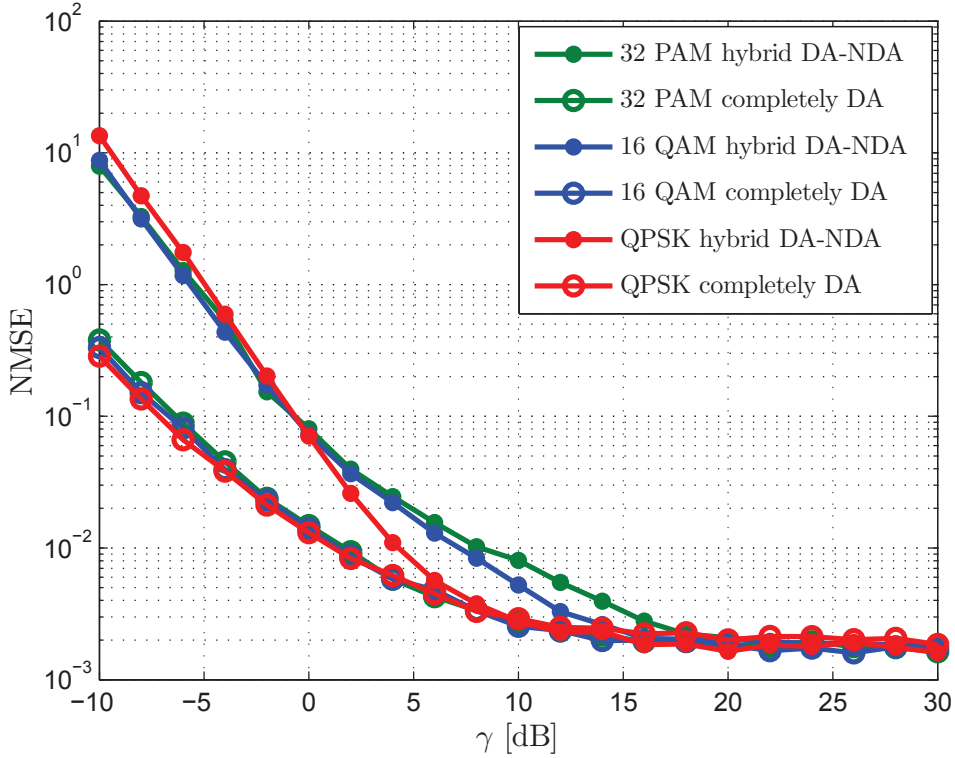


Figure 4.9: NMSE for the unbiased “*hybrid NDA*” and *completely DA* estimators vs. the average SNR, for different constellations types and orders with $N = \bar{N}_{\text{DA}} = 112$, $\bar{N}_{\text{NDA}} = 56$, $N_r = 2$ and $f_D T_s = 7 \cdot 10^{-3}$, and $L = 4$.

Finally, we compare in Fig. 4.9 the NMSE of the “*hybrid NDA*” estimator to the *completely DA* estimator for different constant- and non-constant-envelope constellations. Clearly, the new estimator exhibits comparable performances, for the different modulation orders and types, with a small advantage for the constant-envelope ones at medium SNR levels. Again, with a small fraction of pilot symbols, the “*hybrid NDA*” estimator ultimately provides the best achievable performance by reaching the *completely DA* estimator that assumes all the transmitted symbols to be perfectly known.

Conclusion

In this thesis, we formulated and derived the ML estimator for *instantaneous* SNR estimator over time-varying SIMO channels, using a polynomial-in-time expansion. In the DA scenario, the ML estimator was derived in a closed-form expression. Its bias, its variance as well as the DA Cramér-Rao lower bound (CRLB) were also derived in closed-form. In the NDA case, however, we proposed a solution that is based on the expectation-maximization concept. This iterative NDA estimator is able to find the exact NDA ML SNR estimates within very few iterations. This iterative estimator requires an appropriate initial guess which was obtained by applying the DA estimator on periodically inserted pilot symbols. The new estimator is also applicable to any fading channel. Using computer simulations, we showed that our newly developed estimator is able to reach the optimal performance over a wide SNR range. In particular, it outperforms by far the new SIMO-enhanced version of the only published work on the subject. Finally, the new ML estimator is also applicable to any linear modulation and exhibits almost the same results for different modulation orders and types.

Appendix A

Derivation of FIM elements for complex channels

By recalling that $\mathbf{h}_i = \boldsymbol{\alpha}_i + j\boldsymbol{\beta}_i$ where $\boldsymbol{\alpha}_i$ and $\boldsymbol{\beta}_i$ stands for the real and imaginary parts of \mathbf{h}_i , respectively, we can derive the required partial derivatives of (3.33) as follows:

$$\frac{\partial^2 \ln(P(\mathbf{y}_{\text{DA}}; \boldsymbol{\theta}'))}{\partial \boldsymbol{\alpha}_i \partial \boldsymbol{\alpha}_i^T} = \frac{\partial^2 \ln(P(\mathbf{y}_{\text{DA}}; \boldsymbol{\theta}'))}{\partial \boldsymbol{\beta}_i \partial \boldsymbol{\beta}_i^T} = -\frac{1}{\sigma^2} \mathbf{I}_L \quad (4.6)$$

$$\frac{\partial^2 \ln(P(\mathbf{y}_{\text{DA}}; \boldsymbol{\theta}'))}{\partial \sigma^2 \partial \boldsymbol{\alpha}_i^T} = \frac{1}{2\sigma^4} (2\boldsymbol{\alpha}_i^T - 2\Re\{\mathbf{y}_{i,\text{DA}}^H \mathbf{A}\}) \quad (4.7)$$

$$\frac{\partial^2 \ln(P(\mathbf{y}_{\text{DA}}; \boldsymbol{\theta}'))}{\partial \sigma^2 \partial \boldsymbol{\beta}_i^T} = \frac{1}{2\sigma^4} (2\boldsymbol{\beta}_i^T - 2\Im\{\mathbf{y}_{i,\text{DA}}^H \mathbf{A}\}) \quad (4.8)$$

and

$$\frac{\partial^2 \ln(P(\mathbf{y}_{\text{DA}}; \boldsymbol{\theta}'))}{\partial \sigma^2^2} = \frac{NN_r}{\sigma^4} - \sum_{i=1}^{N_r} \frac{1}{\sigma^6} (\mathbf{y}_{i,\text{DA}} - \mathbf{A}\mathbf{h}_i)^H (\mathbf{y}_{i,\text{DA}} - \mathbf{A}\mathbf{h}_i). \quad (4.9)$$

Moreover, it is easy to verify that:

$$\frac{\partial^2 \ln(P(\mathbf{y}_{\text{DA}}; \boldsymbol{\theta}'))}{\partial \boldsymbol{\beta}_i \partial \boldsymbol{\alpha}_i^T} = \frac{\partial^2 \ln(P(\mathbf{y}_{\text{DA}}; \boldsymbol{\theta}'))}{\partial \boldsymbol{\alpha}_i \partial \boldsymbol{\alpha}_i^T} = \frac{\partial^2 \ln(P(\mathbf{y}_{\text{DA}}; \boldsymbol{\theta}'))}{\partial \boldsymbol{\beta}_i \partial \boldsymbol{\beta}_i^T} = \mathbf{0}_L, \quad (4.10)$$

for $1 \leq i \leq N_r$ and $1 \leq l \leq N_r$ with $i \neq l$. In addition, the expected values of the previously derived partial derivatives with respect to \mathbf{y}_{DA} are given by:

$$\mathbb{E}_{\mathbf{y}_{\text{DA}}} \left\{ \frac{\partial^2 \ln(P(\mathbf{y}_{\text{DA}}; \boldsymbol{\theta}'))}{\partial \boldsymbol{\alpha}_i \partial \boldsymbol{\alpha}_i^T} \right\} = \mathbb{E}_{\mathbf{y}_{\text{DA}}} \left\{ \frac{\partial^2 \ln(P(\mathbf{y}_{\text{DA}}; \boldsymbol{\theta}'))}{\partial \boldsymbol{\beta}_i \partial \boldsymbol{\beta}_i^T} \right\} = -\frac{1}{\sigma^2} \mathbf{I}_L \quad (4.11)$$

$$\mathbb{E}_{\mathbf{y}_{\text{DA}}} \left\{ \frac{\partial^2 \ln(P(\mathbf{y}_{\text{DA}}; \boldsymbol{\theta}'))}{\partial \sigma^2} \right\} = -\frac{NN_r}{\sigma^4}, \quad (4.12)$$

and it can be easily shown that:

$$\mathbb{E}_{\mathbf{y}_{\text{DA}}} \left\{ \frac{\partial^2 \ln(P(\mathbf{y}_{\text{DA}}; \boldsymbol{\theta}'))}{\partial \sigma^2 \partial \boldsymbol{\alpha}_i^T} \right\} = \mathbb{E}_{\mathbf{y}_{\text{DA}}} \left\{ \frac{\partial^2 \ln(P(\mathbf{y}_{\text{DA}}; \boldsymbol{\theta}'))}{\partial \sigma^2 \partial \boldsymbol{\beta}_i^T} \right\} = \mathbf{0}_{1 \times L}. \quad (4.13)$$

Now by using:

$$[\mathbf{I}_{\text{DA}}(\boldsymbol{\theta}')]_{i,l} = -\mathbb{E}_{\mathbf{y}_{\text{DA}}} \left\{ \frac{\partial^2 \ln(P(\mathbf{y}_{\text{DA}}; \boldsymbol{\theta}'))}{\partial \boldsymbol{\theta}'_i \partial \boldsymbol{\theta}'_l^T} \right\} \quad (4.14)$$

we can finally derive the analytical expression for the FIM as follows:

$$[\mathbf{I}_{\text{DA}}(\boldsymbol{\theta}')] = \begin{pmatrix} \frac{1}{\sigma^2} \mathbf{I}_L & \mathbf{0}_L & \cdots & \mathbf{0}_L & \mathbf{0}_{L \times 1} \\ \mathbf{0}_L & \ddots & \ddots & \vdots & \vdots \\ \vdots & \ddots & \ddots & \mathbf{0}_L & \mathbf{0}_{L \times 1} \\ \mathbf{0}_L & \cdots & \mathbf{0}_L & \frac{1}{\sigma^2} \mathbf{I}_L & \mathbf{0}_{L \times 1} \\ \mathbf{0}_{1 \times L} & \cdots & \cdots & \mathbf{0}_{1 \times L} & \frac{NN_r}{\sigma^4} \end{pmatrix} \quad (4.15)$$

which turns out to be block-diagonal whose inverse is straightforward. Finally, by injecting (4.15) and (3.35) in (3.31) and after some algebraic manipulations, a closed-form expression of the CRLB of the DA *instantaneous* SNR estimates is obtained as given by (3.36).

Appendix B

Derivation of the closed-form expression for the estimated symbol matrix \mathbf{A} in the QPSK case

In this appendix, we will detail the derivation of (3.67). Assuming $a(n) \in \{\pm\sqrt{(1/2)} \pm j\sqrt{(1/2)}\}$ (i.e., QPSK transmissions), and given (3.65), it follows:

$$\mathbb{E}\{a(n)|y_i(n); \boldsymbol{\theta}\} = \frac{1}{\sqrt{2}} \frac{\left(\frac{1}{4\pi\sigma^2}\right) \left((\pm 1 \pm j) \exp\left\{\frac{-1}{\sigma^2} \left| y_i(n) - \frac{1}{\sqrt{2}}(\pm 1 \pm j)\hat{h}_i(n) \right|^2\right\} \right)}{\left(\frac{1}{4\pi\sigma^2}\right) \exp\left\{\frac{-1}{\sigma^2} \left| y_i(n) - \frac{1}{\sqrt{2}}(\pm 1 \pm j)\hat{h}_i(n) \right|^2\right\}}, \quad (4.16)$$

which can be rewritten as:

$$\mathbb{E}\{a(n)|y_i(n); \boldsymbol{\theta}\} = \frac{1}{\sqrt{2}} \frac{(\pm 1 \pm j) \exp\left\{\frac{\sqrt{2}}{\sigma^2} \Re\{(\pm 1 \pm j)y_i(n)\hat{h}_i^*(n)\}\right\}}{\exp\left\{\frac{\sqrt{2}}{\sigma^2} \Re\{(\pm 1 \pm j)y_i(n)\hat{h}_i^*(n)\}\right\}}. \quad (4.17)$$

Then, after some rearrangements, (4.17) reduces to:

$$\mathbb{E}\{a(n)|y_i(n); \boldsymbol{\theta}\} = \frac{1}{\sqrt{2}} \frac{(1+j) \sinh\left\{\frac{\sqrt{2}}{\sigma^2} \Re\{(1-j)y_i(n)\hat{h}_i^*(n)\}\right\} + (1-j) \sinh\left\{\frac{\sqrt{2}}{\sigma^2} \Re\{(1+j)y_i(n)\hat{h}_i^*(n)\}\right\}}{\cosh\left\{\frac{\sqrt{2}}{\sigma^2} \Re\{(1-j)y_i(n)\hat{h}_i^*(n)\}\right\} + \cosh\left\{\frac{\sqrt{2}}{\sigma^2} \Re\{(1+j)y_i(n)\hat{h}_i^*(n)\}\right\}}. \quad (4.18)$$

And finally, we obtain the result given in (3.67):

$$[\widehat{\mathbf{A}}]_{mn}^H = \frac{1}{\sqrt{2}} \left[\tanh \left\{ \frac{\sqrt{2}}{\widehat{\sigma}^2} \Re \{ y_i(n) \widehat{h}_i^*(n) \} \right\} - j \tanh \left\{ \frac{\sqrt{2}}{\widehat{\sigma}^2} \Im \{ y_i(n) \widehat{h}_i^*(n) \} \right\} \right]. \quad (4.19)$$

Bibliography

- [1] N. C. Beaulieu, A. S. Toms, and D. R. Pauluzzi, "Comparison of four SNR estimators for QPSK modulations," *IEEE Commun. Lett.*, vol. 4, pp. 43-45, Feb. 2000.
- [2] K. Balachandran, S. R. Kadaba, and S. Nanda, "Channel quality estimation and rate adaption for cellular mobile radio," *IEEE J. Sel. Areas Commun.*, vol. 17, no. 7, pp. 1244-1256, July 1999.
- [3] T. A. Summers and S. G. Wilson, "SNR mismatch and online estimation in turbo decoding," *IEEE Trans. Commun.*, vol. 46, no. 4, pp. 421-423, Apr. 1998.
- [4] N. Nahi and R. Gagliardi, "On the estimation of signal-to-noise ratio and application to detection and tracking systems," University of Southern California, Los Angeles, EE Report 114, July 1964.
- [5] T. Benedict and T. Soong, "The joint estimation of signal and noise from sum envelope," *IEEE Trans. Inf. Theory*, vol. 13, pp. 447-457, July 1967.
- [6] D. R. Pauluzzi and N. C. Beaulieu, "A comparison of SNR estimation techniques for the AWGN channel," *IEEE Trans. Commun.*, vol. 48, pp. 1681-1691, Oct. 2000.

- [7] M. Turkboylari and G. L. Stuber, "An efficient algorithm for estimating the signal-to-interference ratio in TDMA cellular systems," *IEEE Trans. Commun.*, vol. 46, no. 6, pp. 728-731, June 1998.
- [8] P. Gao and C. Tepedelenlioglu, "SNR estimation for non-constant modulus constellations," *IEEE Trans. Signal Process.*, vol. 53, no. 3, pp. 865-870, March 2005.
- [9] R. Lopez-Valcarce and C. Mosquera, "Sixth-order statistics-based non-data-aided SNR estimation," *IEEE Commun. Lett.*, vol. 11, no. 4, pp. 351-353, Apr. 2007.
- [10] M. Álvarez-Díaz, R. López Valcare, and C. Mosquera "SNR estimation for multilevel constellations using higher-order moments," *IEEE Trans. Signal Process.*, vol. 58, no. 3, pp. 1515-1526, Mar. 2010.
- [11] A. Stéphenne, F. Bellili, and S. Affes, "Moment-based SNR estimation over linearly-modulated wireless SIMO channels," *IEEE Trans. Wireless Commun.*, vol. 9, no. 2, pp. 714-722, Feb. 2010.
- [12] A. Stéphenne, F. Bellili, and S. Affes, "Moment-based SNR estimation for SIMO wireless communication systems using arbitrary QAM," in *Proc. 41st Asilomar Conference on Signals, Systems and computers*, pp. 601-605, Nov. 2007.
- [13] A. Das (Nandan), "NDA SNR estimation: CRLB and EM based estimators", in *Proc. IEEE TENCON'08*, pp. 1-6, Nov. 2008, Hyderabad, India.
- [14] M. A. Boujelben, F. Bellili, S. Affes, and A. Stephenne, "SNR estimation over SIMO channels from linearly modulated signals," *IEEE Trans. Signal Process.*, vol. 58, no. 12, pp. 6017-6028, Dec. 2010.

- [15] A. Das and B. D. Rao, "SNR and noise variance estimation for MIMO systems," *IEEE Trans. Signal Process.*, vol. 60, no. 8, pp. 3929-3941, Aug. 2012.
- [16] G. L. Stüber, *Principles of Mobile Communication*, Boston, MA: Kluwer, 1996.
- [17] T. Gao and B. Sun, "A high-speed railway mobile communication system Based on LTE," in *Proc. ICEIE 2010*, vol. 1, pp. 414-417, Aug. 2010, Kyoto, Japan.
- [18] A. Wiesel, J. Goldberg, and H. Messer-Yaron, "SNR estimation in time-varying fading channels," *IEEE Trans. Commun.*, vol. 54, no. 5, May 2006.
- [19] F. Bellili, A. Stéphenne and S. Affes, "SNR estimation of QAM-modulated transmissions over time-varying SIMO channels," *IEEE ISWCS'08*, pp. 199-203, Oct. 2008, Reykjavik, Iceland.
- [20] S. M. Kay, *Fundamentals of Statistical Signal Processing-Estimation Theory*. Englewood Cliffs, NJ: Prentice-Hall, 1993.
- [21] A.P. Dempster, N.M. Laird, and D.B. Rubin, "Maximum likelihood from incomplete data via the EM algorithm," *Journal of the Royal Statistical Society, Series B*, no. 1, pp. 1-38, 1977.
- [22] C. Anton-Haro, J. A. R. Fonollosa, C. Fauli, and J. R. Fonollosa, "On the inclusion of channel's time dependence in a hidden Markov model for blind channel estimation," *IEEE Trans. Veh. Technol.*, vol. 50, no. 3, pp. 867-873, May 2001.
- [23] S. M. Kay, *Fundamentals of Statistical Signal Processing-Detection Theory*. Englewood Cliffs, NJ: Prentice-Hall, 1998.
- [24] 3GPP TS 36.211: 3rd Generation Partnership Project; Technical Specification Group Radio Access Network; Evolved Universal Terrestrial Radio Access (E-UTRA); Physical Channels and Modulation.